Optimisation of supercritical extractions of C4 biomasses and Fractionation of sugarcane.

Sunlibb deliverable 6.2 and CePRObio/Sunlibb joint deliverable 6.2

Dr. Andrew Hunt & Thomas Attard

University of York

01/02/2013

Abstract

The optimisation of the extraction of epicuticular waxes from C4 biomasses was achieved using the factorial experimental design. The extraction yield is the response variable and the two factors which were chosen as the independent variables were temperature and pressure. The effect of temperature and pressure on the extraction yield was modelled using the dimensionless factor coordinate system. The initial set of experiments was carried out over four hour extraction periods. A variety of temperature and pressure ranges were incorporated in this study. The optimal conditions for *miscanthus* giganteus were found to be 350 bar and 50 ^{o}C. For maize, the optimal conditions were found to be 400 bar and 65 ^{o}C while the optimal conditions for sugarcane bagasse were found to be 325 bar and 57 ^{o}C. Results indicate that for miscanthus and sugarcane bagasse, density plays a more important role than temperature in the extraction of waxes. Furthermore, in both cases, the results suggest that a specific density is requited for optimal extraction. In the case of maize, results indicate that temperature is more important than density in the extraction of waxes.

In addition to optimisation, fractionation of sugarcane bagasse and sugarcane leaves is reported. The sugarcane bagasse was fractionated using a number of different fractional separators set at different pressures and temperatures, each having a different pressure. The fractionation of sugarcane leaves was attempted by a combination of complementary chromatographic techniques, namely TLC and flash chromatography.

1. Aim

To optimise the extraction of epicuticular waxes from C4 biomasses (miscanthus, maize and sugarcane bagasse) using the factorial experimental design. This work also demonstrates the potential to fractionate into higher value components. Samples of sugarcane leaves and stems were obtained during a student exchange visit to the University of Sao Paulo (USP) between March to May 2012 and optimisations were conducted at the University of York.

2. Introduction

2.1 Supercritical Fluids

A supercritical fluid refers to a substance that has its pressure and temperature above their critical point values (P_c, T_c).[1-3] The physical properties of a substance change when varying the temperature and pressure. This phenomenon can be explained with the aid of a phase diagram, which is essentially a plot of vapour pressure vs temperature (Figure 2.1).[4]

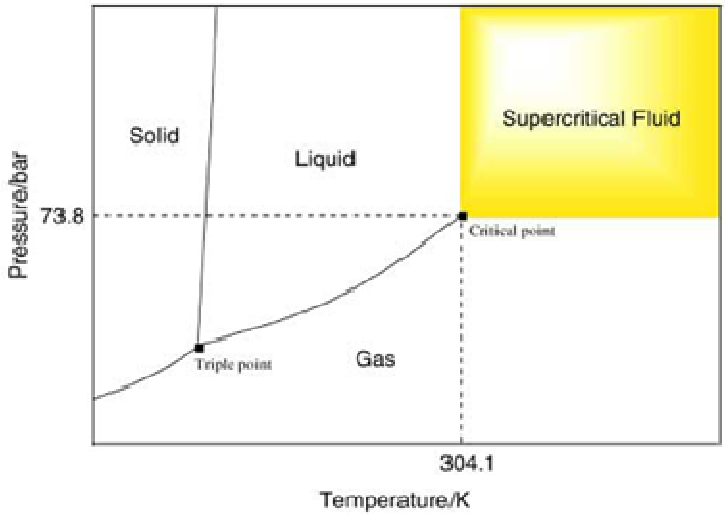

Figure 2.1 Phase diagram for carbon dioxide.[4]

All stable compounds have a triple point and critical point.[5] The triple point represents the temperature and pressure at which the three phases are in equilibrium with one another and can therefore coexist. The line found lying between the liquid and gas region represents the gas-liquid coexistence curve.[6] When moving along the gas-liquid coexistence curve, towards the critical point, the density of the liquid phase decreases due to thermal expansion while the density of the gas phase increases due to the increase in pressure.[6] At the critical point, the density of the liquid phase becomes equivalent to the density of the gas phase resulting in identical properties and thus it is no longer possible to distinguish between the two phases.[4,6] The critical point represents the maximum temperature and pressure that can be applied where a substance can be found as a liquid and a gas in equilibrium with each other. Increasing the temperature and pressure beyond the critical point terminates the gas/liquid equilibrium, where the substance no longer behaves as a liquid or a gas.[4] The above phase diagram is for carbon dioxide, in which the critical point is found at 73.8 bar and 31.1 ^{o}C.[2]

2.1.1 Supercritical fluids: Physical Properties

The range in which the most interesting SCF applications occur is $1< T/T_c <1.1$ and $1< P/P_c <2$. When in this range, SCFs are in a single condensed phase and have properties between

those of a gas and a liquid.[1] Slight changes in temperature and pressure could lead to a significant variation in these physical properties.[2]

It has been demonstrated by a variety of different authors that the "logarithm of solubility is approximately linearly dependent on the solvent density".[7-11] A number of experiments involving hydrocarbons demonstrated that there is an exponential variation in hydrocarbon solubility with a change in density of the supercritical fluid (supercritical CO_2, ethane or ethylene).[10-13] Slight adjustments to the temperature and pressure lead to a significant change in solvent density which in turn causes variations in the density-dependent solvent properties such as the partition coefficient, solubility parameter and dielectric constant.[14]

In addition, apart from solubility, other factors which influence the solvent power of supercritical fluids are diffusivity and viscosity.[61] Table 2.1 summarises the densities, viscosities and diffusion coefficients of a solid, liquid and supercritical fluid. From the Table 2.1 it can be seen that the viscosity of a supercritical fluid is generally an order of magnitude lower than the viscosity of a liquid while the diffusivity is an order of magnitude higher.[15,16] Therefore this leads to enhanced heat and mass transfer.[17]

Table 2.1 Thermophysical properties of the three fluid states.

Fluid State	Density (kg m^{-3})	Viscosity (N s m^{-2})	Diffusion Coefficient (m^2 s^{-1})
Liquid	800 – 1200	10^{-3} – 10^{-2}	10^{-8} – 10^{-9}
Supercritical fluid	250 – 800	10^{-4} – 10^{-3}	10^{-7} – 10^{-8}
Gas	1 – 100	10^{-5} – 10^{-4}	10^{-4} – 10^{-5}

It was suggested by Dobbs and Johnston that there is a phenomenon referred to as an entrainer effect, whereby there is a greater solubility enhancement with the presence of solutes in the supercritical phase that act as co-solvents.[18] They measured the solubilities for binary, ternary and quartenary systems, consisting of supercritical CO_2, a co-solvent and combinations of solid phases. It was suggested that in ternary systems, involving two solutes and the supercritical phase, there is a proportional increase in the solubility of one solute in the system relative to the solubility of the second solute. Therefore an entraining effect occurs (as a result of the more soluble solute) which leads to the enhancement of the less soluble

solvent. Therefore this indicates that the addition of compounds into supercritical fluids results in a change in the solvent properties.[18]

Furthermore, Dobbs *et al*. noted that the addition of small amounts of various co-solvents led to a marked improvement in the selectivity of a nonpolar supercritical fluid solvent for polar vs non polar solids.[18,19] The addition of several mole percent of various cosolvents led to enhanced solubility of certain solids in supercritical carbon dioxide. There was an increase in the solubility of 2-aminobenzoic acid by 620% with only 3.5 mol. % methanol.[19]

2.2 Optimisation of operating conditions: a statistical approach

As stated previously, the main purpose of this work was to attempt to optimise the % yield of wax extracted from the different biomasses by varying parameters which would affect the extraction potential of supercritical carbon dioxide. The extraction yield was optimised by applying the factorial experimental design.

Experimental designs are an efficient way to enhance the value of research and cut down the time which is allotted for process development.[20] Factorial experimental design is a tool which enables the identification of optimal conditions for extractions. A factor refers to any aspect of the experimental conditions that has a direct effect on the result obtained from an experiment.[20,21]

Factorial experimental design aids to construct a mathematical model in order to describe relationships which may exist between variables. Normally, just one variable is of interest, referred to as the response (or dependent) variable which is dependent on a set of variables called explanatory (or independent) variables.

In this case the response variable is the extraction yield. In analytical supercritical fluid extraction, the main explanatory variables include pressure, temperature, density flow rate, duration of the extraction and biomass preparation. The explanatory factors which were investigated were temperature and pressure and these were varied according to the requirement of the experiment. The other independent variables were kept constant throughout the investigation.

3. Results and Discussion

The independent factors, pressure and temperature, were investigated at two levels, referred to as a two-level factorial design. This requires 2^f runs in which each factor is at two levels, those of the minimum and maximum extraction limits.

The effect of temperature and pressure on the extraction yield was modelled using the dimensionless factor coordinate system (Figure 3.1). The initial set of experiments was carried out over four hour extraction periods. A variety of temperature and pressure ranges were incorporated into this study as seen in Table 3.1.

Table 3.1 Experimental design for optimisation process

Experiment	Temperature	Pressure
1	High	High
2	High	Low
3	Low	High
4	Low	Low
5	Medium	Medium

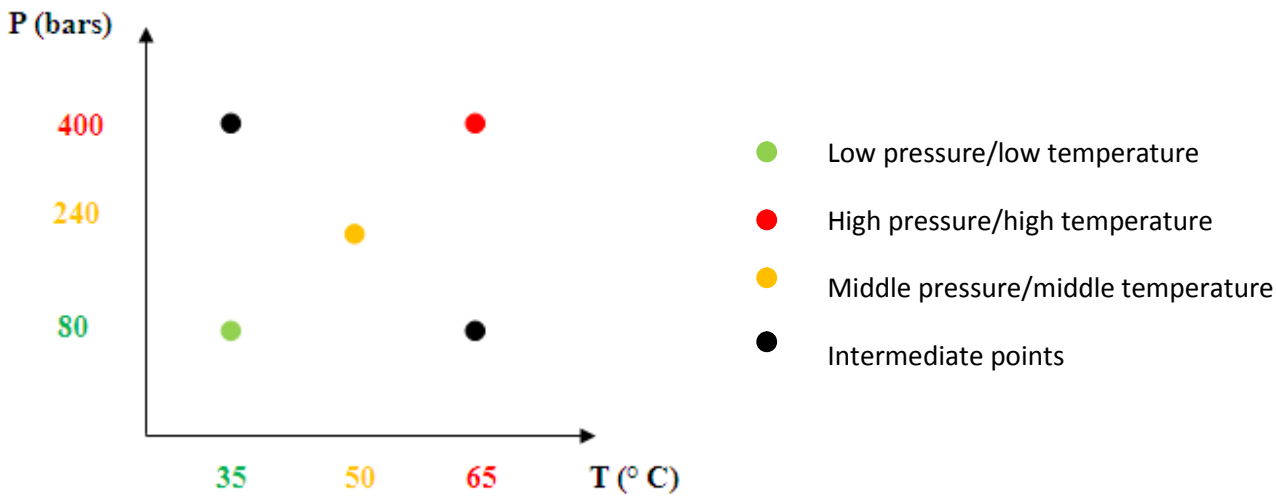

Figure 3.1 Experimental Design for optimisation process.

As stated previously, it is known that there is a relationship between the extraction capability of supercritical carbon dioxide and its density. It was therefore predicted that an increase in

the density of carbon dioxide would lead to an increase in extraction yield. However, results show that each biomass had its own set of optimal extraction conditions.

3.1 Miscanthus

Table 3.2 % Extraction yields obtained at different pressures and temperatures for *miscanthus giganteus.*

Experiment	Temperature (^{o}C)	Pressure (bar)	Extraction Yield (%)
1	35	80	0.43
2	65	80	0.014
3	50	240	1.27
4	35	400	1.32
5	65	400	1.74
6	50	350	1.96

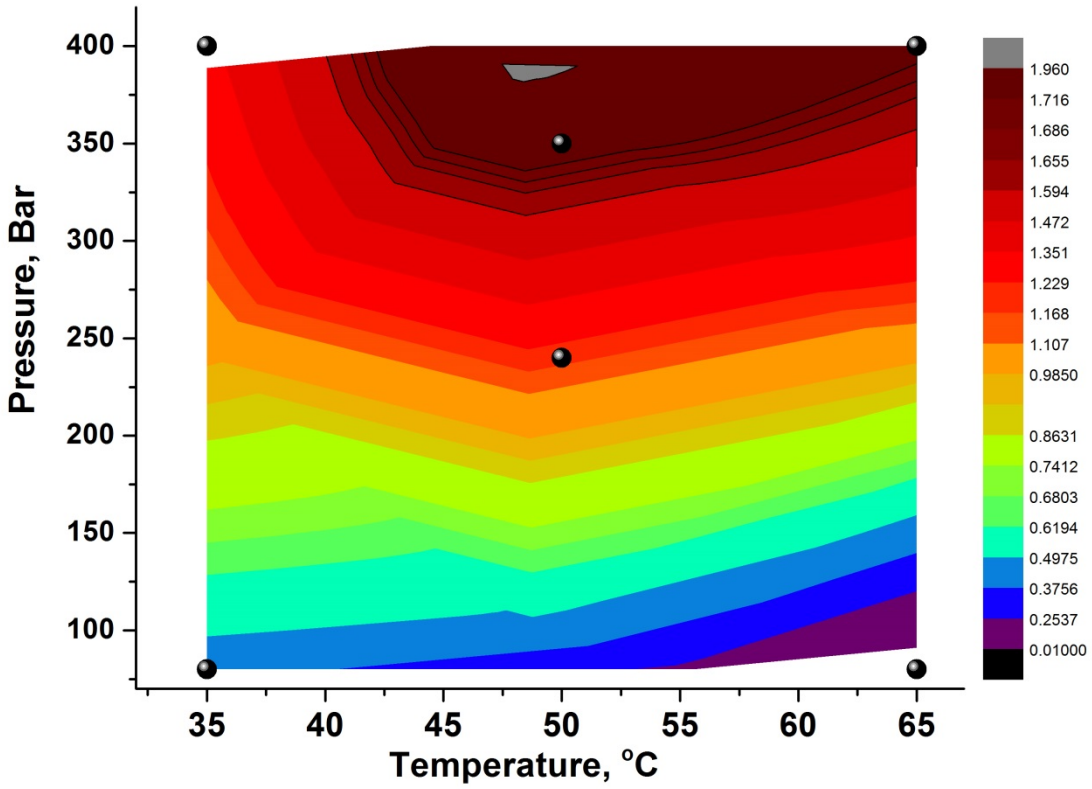

Figure 3.2 % crude yield of *miscanthus giganteus* waxes from supercritical extraction.

The extraction yields for the different experiments are summarised in Table 3.2. These results have shown that the highest extraction yield was obtained when a pressure of 350 bar and temperature of 50 ^{o}C were implemented. The density of carbon dioxide at this temperature and pressure is higher than the extraction that took place at an elevated temperature and pressure (400 bar, 65 ^{o}C) which suggests that in the case of miscanthus, density plays a more important role in extraction of waxes from miscanthus than temperature. However, there is an optimal temperature and pressure which gives a density of 899.23 kg/m^3, that results in the highest extraction yields of wax from *miscanthus giganteus*. This suggests that there is a specific density of carbon dioxide that is essential for the extraction of waxes from *miscanthus giganteus*. Very low yields of wax were extracted when carrying out the extractions at low pressure.

3.2 Maize

Table 3.3 % Extraction yields obtained at different pressures and temperatures for maize.

Experiment	Temperature (^{o}C)	Pressure (bar)	Extraction Yield (%)
1	35	80	0.33
2	65	80	0.024
3	50	240	0.91
4	35	400	0.71
5	65	400	1.71
6	50	350	1.02

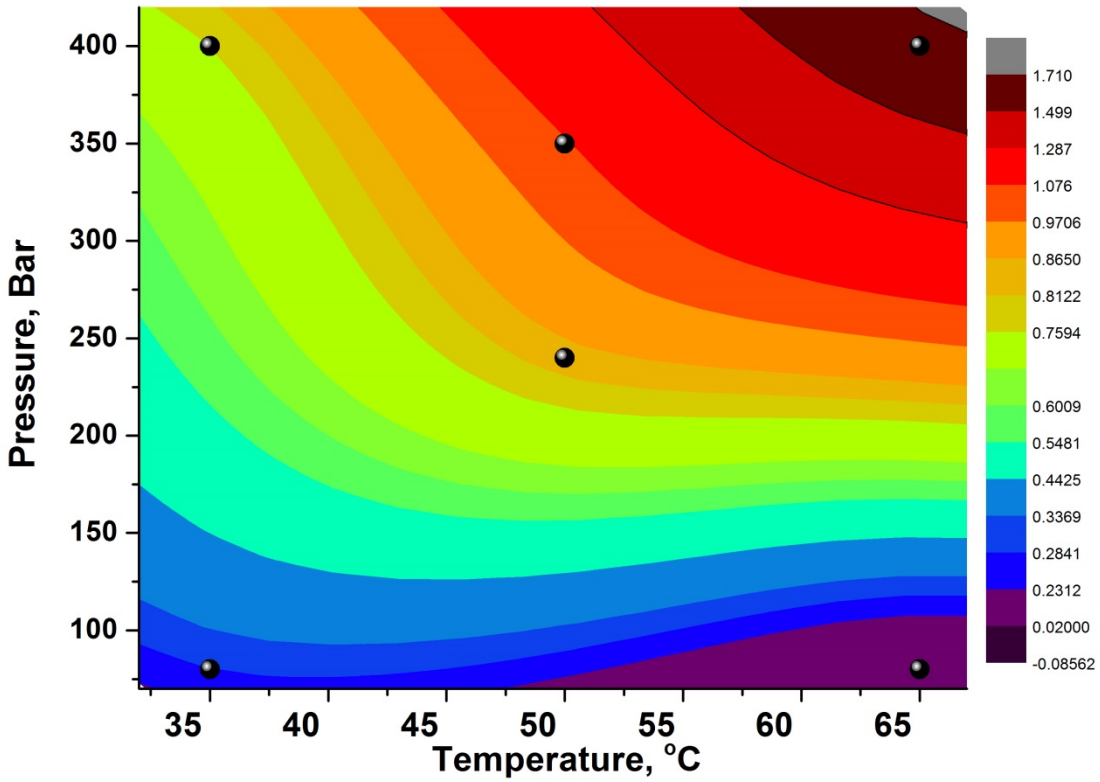

Figure 3.3 % crude yield of maize waxes from supercritical extraction.

In the case of maize, the greatest extraction yield (1.71%) was obtained when the most extreme conditions (400 bar and 65 ^{o}C) implemented. This is significantly higher than the % yield (1.02%) obtained when the extraction was carried out at 350 bar and 50 ^{o}C. When carrying out the extraction at this temperature and pressure, the density of carbon dioxide is lower than when the extractions are carried out at 350 bar and 50 ^{o}C. This indicates that high temperature and pressure have a positive and dramatic effect on the supercritical extraction of wax from maize. In contrast to *miscanthus giganteus*, this suggests that temperature has a more significant effect than density in the extraction of waxes from maize. Similarly to miscanthus, very small yields of wax were extracted when carrying out the extractions at low pressure.

3.3 Sugarcane bagasse

Table 3.4 % Extraction yields obtained at different pressures and temperatures for sugarcane bagasse.

Experiment	Temperature (^{o}C)	Pressure (bar)	Extraction Yield (%)

1	35	80	0.17
2	65	80	0.05
3	65	80	0.06
4	50	240	0.51
5	50	240	0.48
6	57	325	0.66
7	35	400	0.38
8	65	400	0.51
9	50	350	0.42
10	50	350	0.43

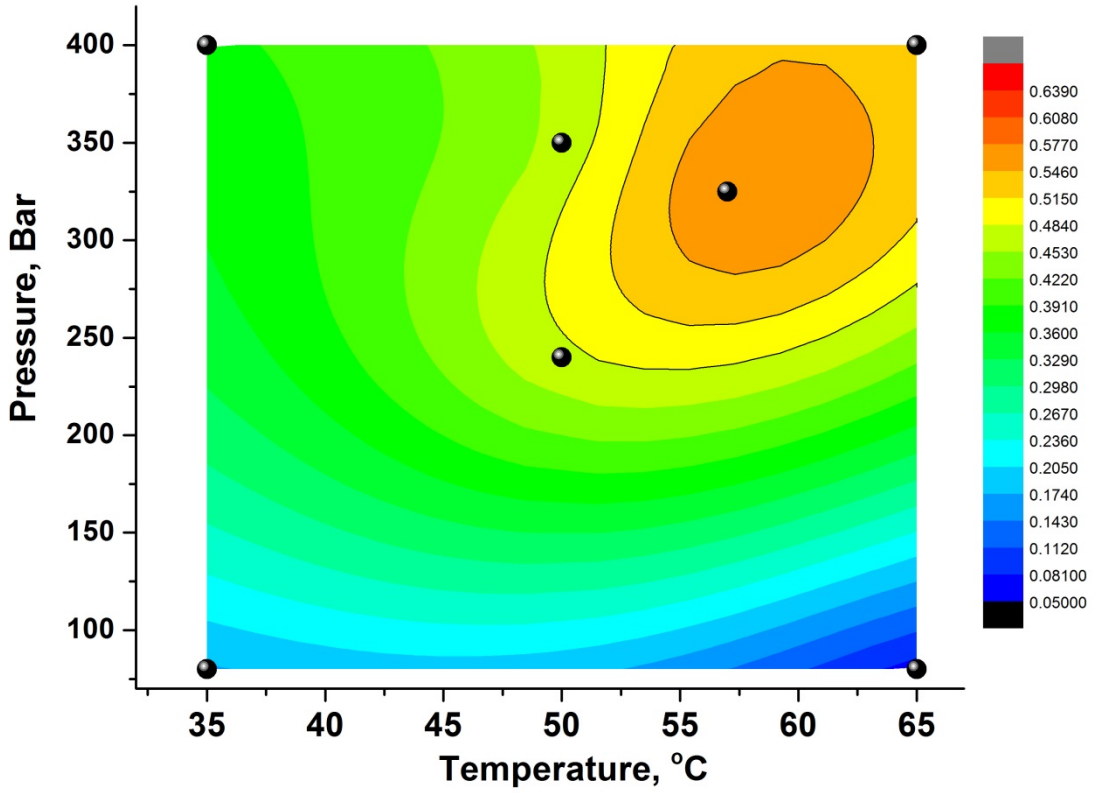

Figure 3.4 % crude yield of sugarcane bagasse waxes from supercritical extraction.

Table 3.4 shows the % yields of wax extracted from sugarcane bagasse under different temperatures and pressures. The maximum yield was achieved with a pressure of 325 bar and temperature of 50 ^{o}C. Similar to *miscanthus giganteus*, these results suggest that a specific density (858.83 kg/m^{3}) is needed for the maximal extraction of wax from sugarcane bagasse

since the highest yield was achieved with a specific set of conditions. Differences within the three optimised conditions are likely to be due to compositional differences within the plants.

3.4 Fractionation of sugarcane bagasse

A potential method for fractionating at the point of extraction was attempted using the wax extracted from sugarcane bagasse. The wax was loaded into the extractor which was set at 350 bar and 50 ^{o}C. Supercritical carbon dioxide was pumped through at a flow rate of 40 g/min and the wax was collected in four fractional separators which were set a: a) 250 bar and 50 ^{o}C b) 150 bar and 50 ^{o}C c) 75 bar and 35 ^{o}C and d) atmospheric pressure and temperature. This can be seen in Figure 3.5 above.

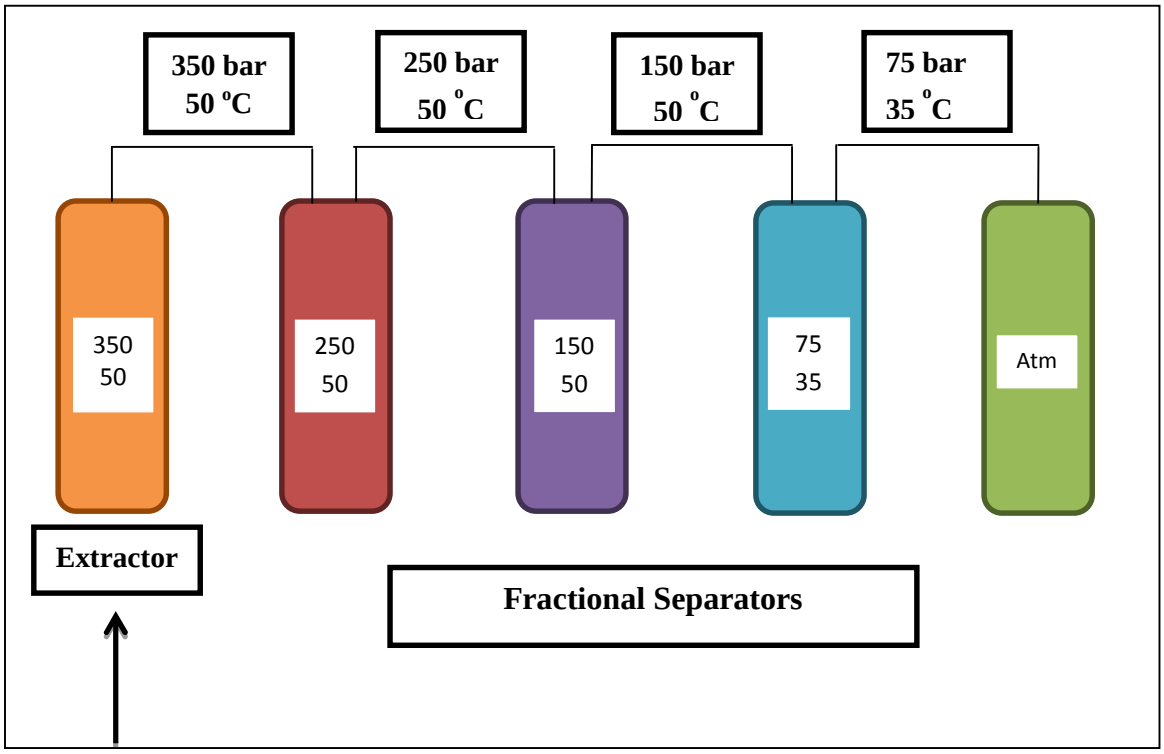

Figure 3.5 Fractionation of sugarcane bagasse experimental set-up.

Figure 3.6 shows the composition of wax collected from each fractional separator. It can be seen that at higher pressures (250 bar and 150 bar) there are larger concentrations of wax esters than at lower pressures (150 bar and atmospheric pressure). At lower pressures there

are higher concentrations of fatty acids. This fractionating method is ideal for obtaining waxes that have different melting points.

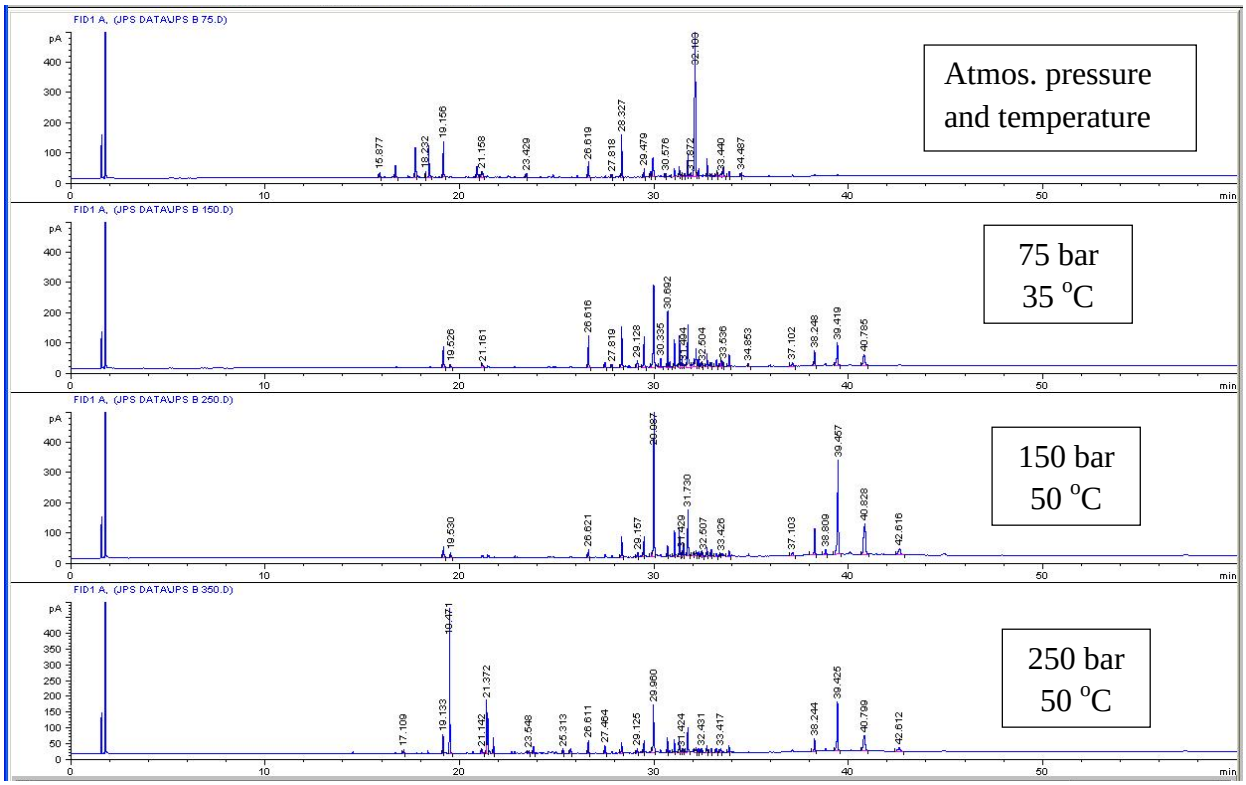

Figure 3.6 GC chromatogram illustrating the composition of wax found in each fraction

3.5 Fractionation of sugarcane leaves.

An attempt was made to fractionate the wax that was extracted from sugarcane leaves using a combination of complementary chromatographic techniques including TLC, flash chromatography and GC. The primary aim was to try and isolate the triterpenoid fraction, which will be discussed later on.

TLC was used in order to find a suitable solvent system to carry out the fractionation. A hexane : ethyl acetate solvent system with a ratio of 3:1 was found to give adequate separation of the various groups of compounds making up the sugarcane wax. This solvent system was selected and used in order to separate the various groups of compounds via flash chromatography.

Figure 3.7 is a photograph illustrating the fractionation of the different components making up sugarcane wax. Since a silica column was used for the fractionation, the non-polar components elute out first (hydrocarbons) followed by the more polar constituents. Different fractions contained different groups of molecules, which are labelled in the photograph. These groups of compounds were identified by TLC and GC. The different fractions were collected in test tubes as shown in Figure 3.8.

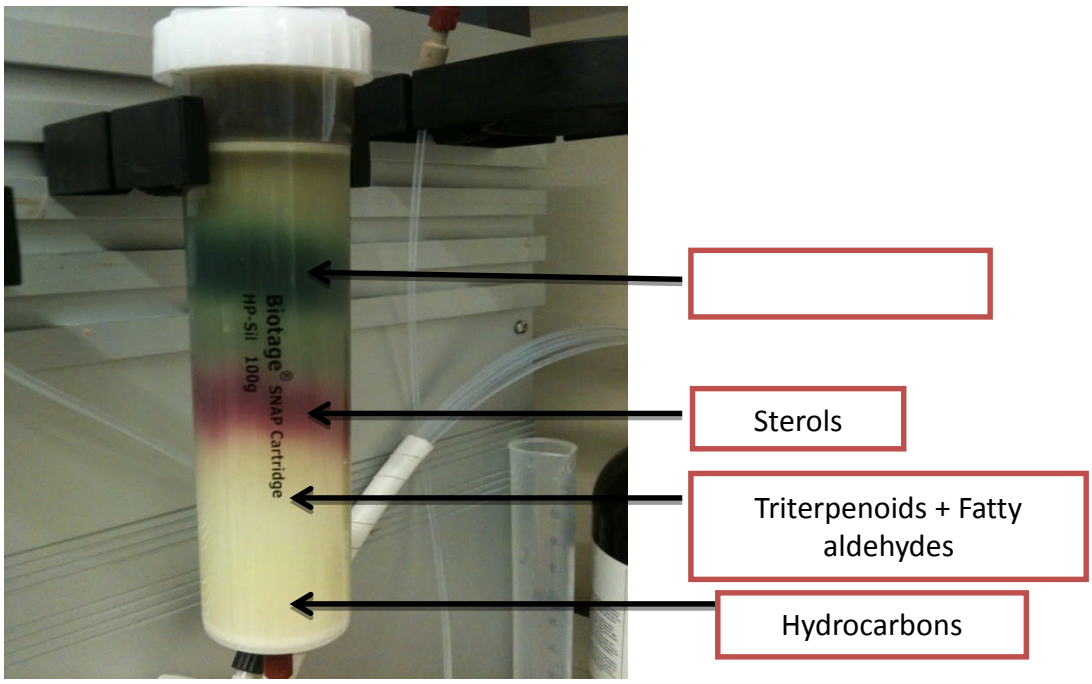

Figure 3.7 Photograph showing the fractionation of the different groups making up the sugarcane wax.

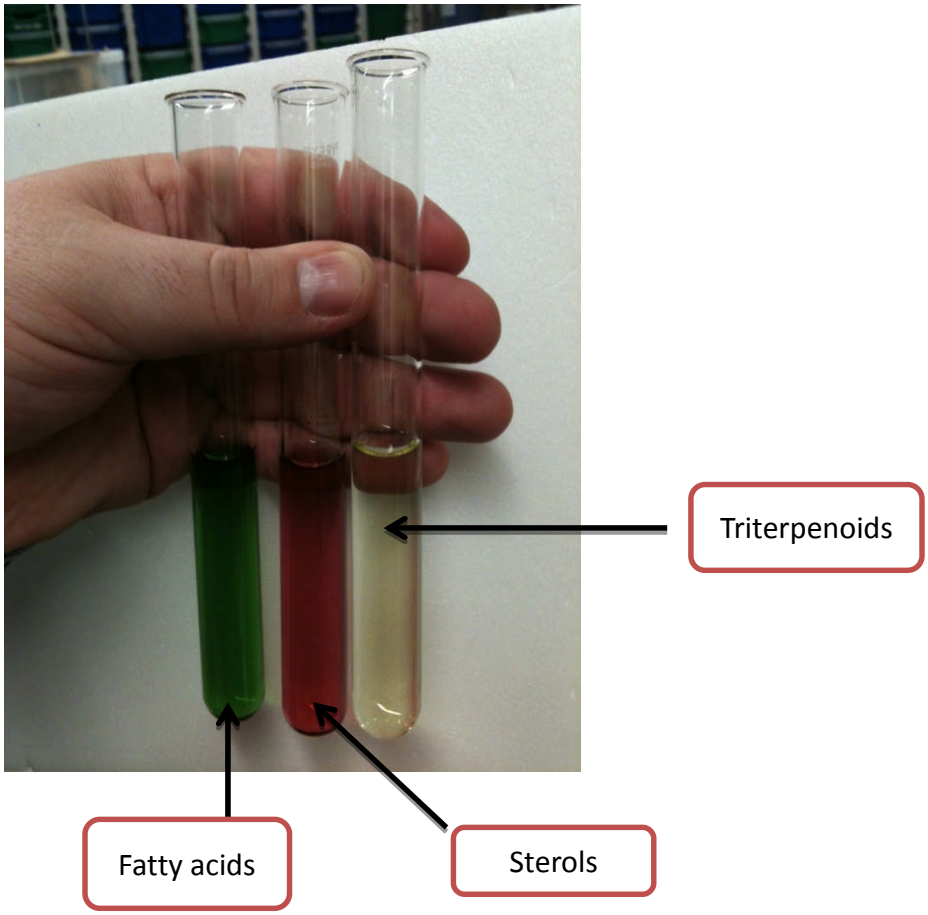

Figure 3.8 Tubes containing a) Fatty acids b) Sterols and c) Triterpenoids.

Figure 3.9 is the GC chromatogram of the wax extracted from sugarcane leaves prior to the fractionation via flash chromatography. A variety of different groups of compounds are found including long-chain hydrocarbons, alcohols, aldehydes, acids (saturated and unsaturated), sterols and triterpinoids.

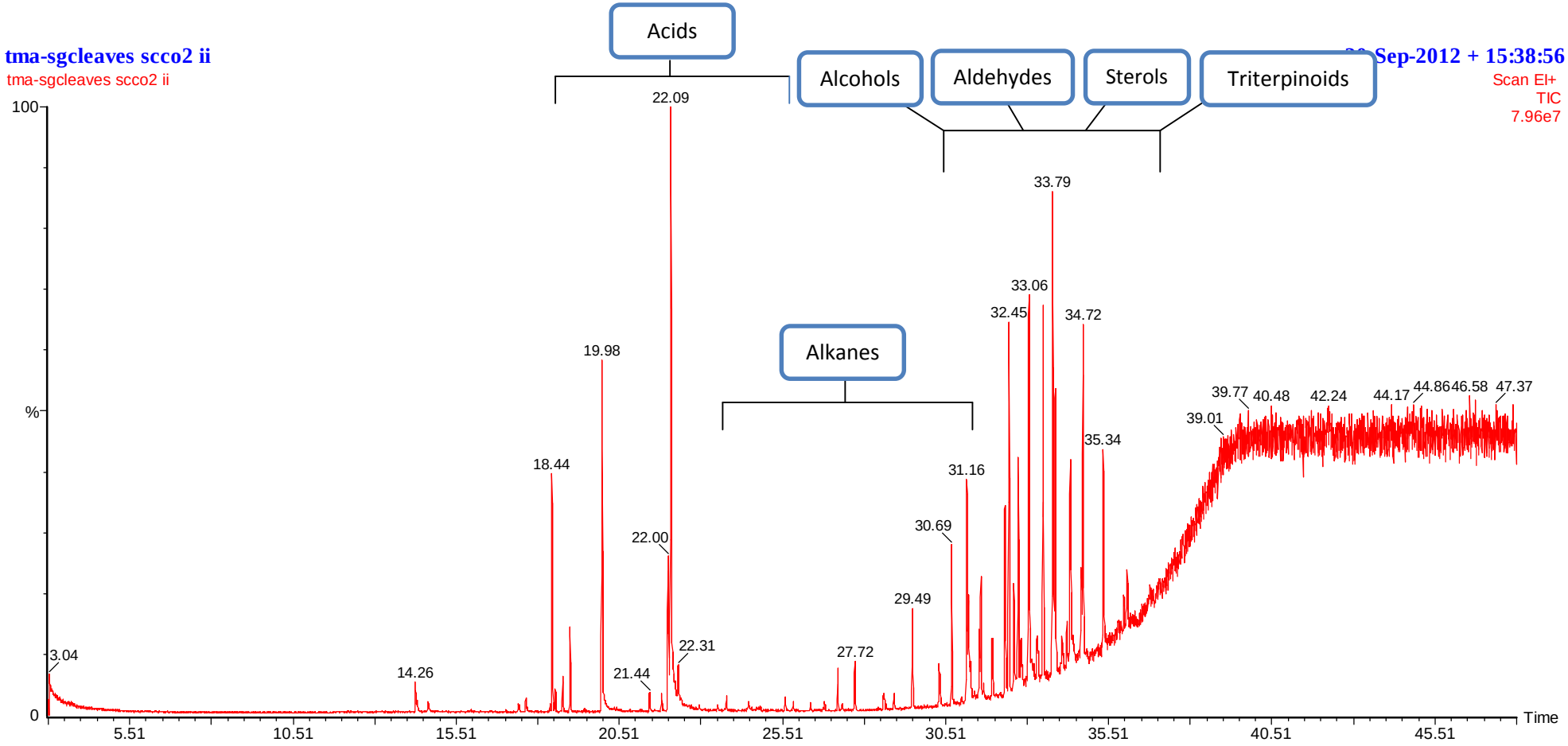

Figure 3.9 GC chromatogram of wax extracted from the leaves of sugarcane prior to fractionation via flash chromatography.

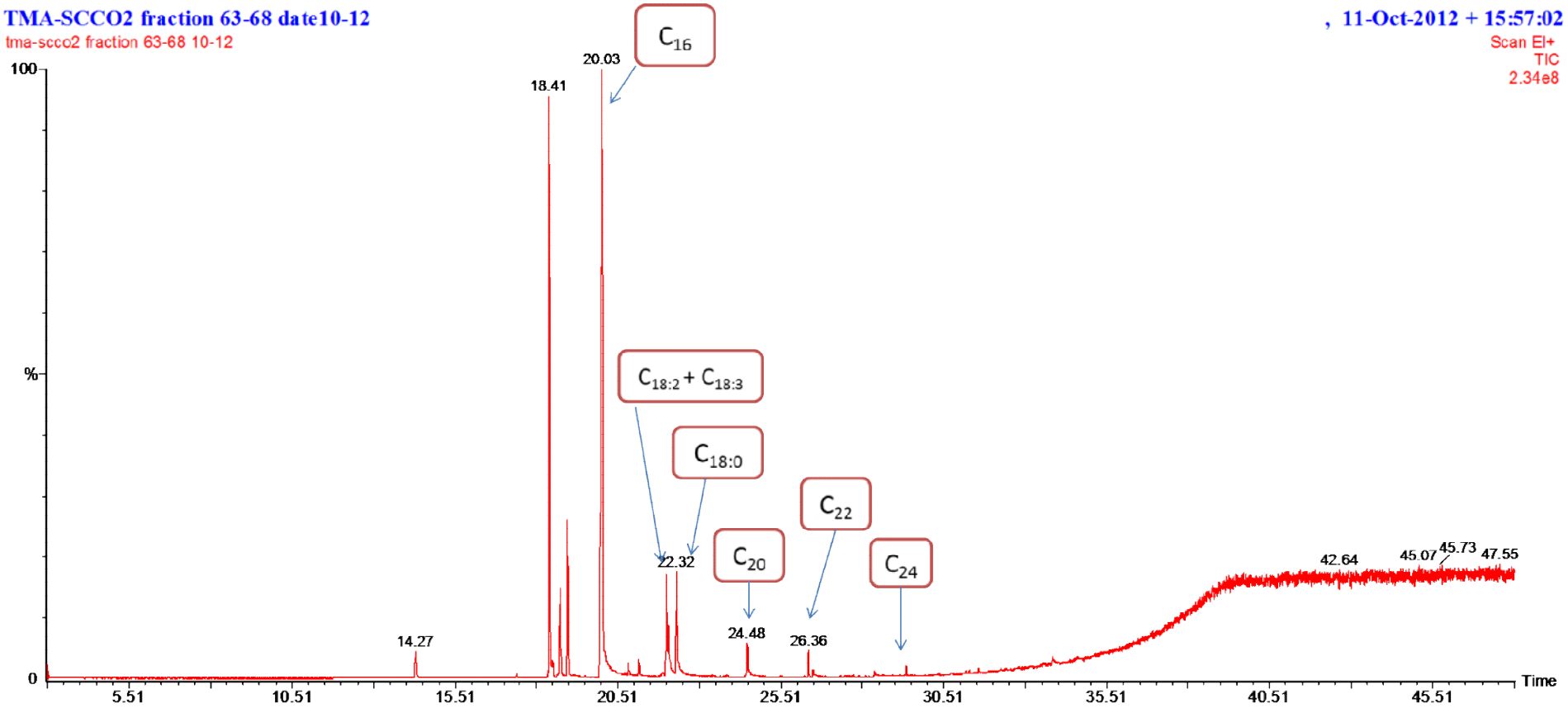

Figure 3.10 GC chromatogram of sugarcane fraction containing the long-chain fatty acids.

3.5.1 Fatty acid fraction

Figure 3.10 is a GC chromatogram illustrating the successful fractionation of the long-chain fatty acids from the crude wax. Four saturated fatty acids were identified having chain lengths varying from C_{16} to C_{24}. Two C_{18} unsaturated fatty acids were identified (C18:2) and (C18:3). The fraction is relatively pure with a few impurities found at around 14 minutes and 18 minutes.

3.5.2 Sterol fraction

Figure 3.11 is a GC chromatogram which shows the successful separation and isolation of the three sterols (β-sitosterol, campesterol and stigmasterol) that are found in sugarcane from the remainder of the wax.

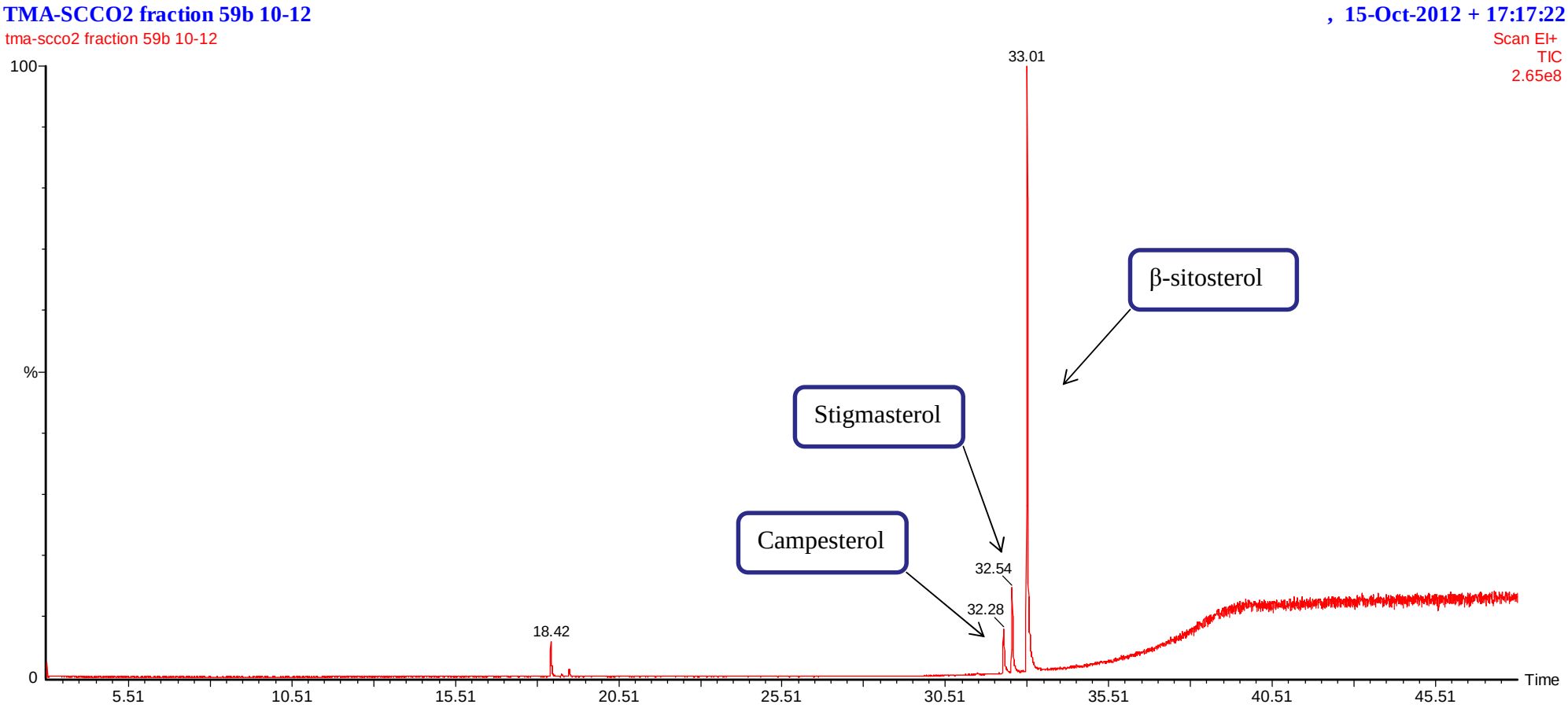

Figure 3.11 GC chromatogram of sugarcane fraction containing the three sterols.

3.5.3 Triterpenoid Fraction

It is very difficult to identify the triterpenoid compounds found in wax extracts as the majority of plants contain a large number of different triterpinoids that are very similar structurally and have similar polarities. In addition a number of them are isomers which makes their separation all the more difficult. The sensitivity of UV detection is very low as triterpenoids lack chromophores, which therefore limits the choice of mobile phase.

The determination of triterpenoids found in the wax extracts of sugarcane was attempted by fractionation of the crude wax and isolation of the triterpenoid fractions. This was done using a combination of complementary chromatographic techniques including TLC, flash chromatography and GC. Triterpenoid fractions which were relatively pure were collected. Structural analysis of the isolated triterpinoids was carried out by means of GC, EI-mass spectrometry, ^{1}H NMR and ^{13}C NMR. Although the fractions collected were not of high purity and some impurities were present in the NMR spectra, the fractions were of adequate purity in order to predict their structure.

From interpretation of the EI-mass spectrum of the crude wax, a considerable number of triterpinoids were found in the leaves. Around five peaks in the spectrum had fragmentation patterns which resemble the fragmentation patterns of triterpinoids.

Two of these compounds were successfully isolated from the rest and were of enough purity to carry out ^{1}H and ^{13} C NMR:

3.5.3.1 Friedelin

One triterpinoid found in the leaves which was successfully isolated from the other triterpinoids as well as the rest of the crude wax (Figure 3.12), was identified as friedelin. A pure standard of friedelin was purchased and therefore a direct comparison was made between the pure standard and the compound found in the leaves.

3.5.3.1.1 GC-MS

The GC retention times of the unknown compound and the pure standard were found to be the same (Figure 3.12). Figure 3.13 compares the EI-mass spectrum of the pure standard and the unknown compound. It can be noted that the two spectra are almost identical. In the EI-mass spectrum of the unknown compound, a number of fragmentation patterns characteristic of friedelin can be identified. The compound showed a molecular ion peak of 426, which is

the molecular weight of friedelin. Diagnostic peaks found at 411, 341, 273, 205 and 123 were present in the spectrum. The peak at 411 occurs as a result of the loss of a methyl group from the molecular ion. The ions with a *m/z* of 341, 273 205 and 123 arise due to the fragmentation of rings A, B, C and D respectively as shown in Scheme 3.1. Therefore the GC-MS data gives strong evidence to suggest that the compound found in the sugarcane leaves is friedelin.

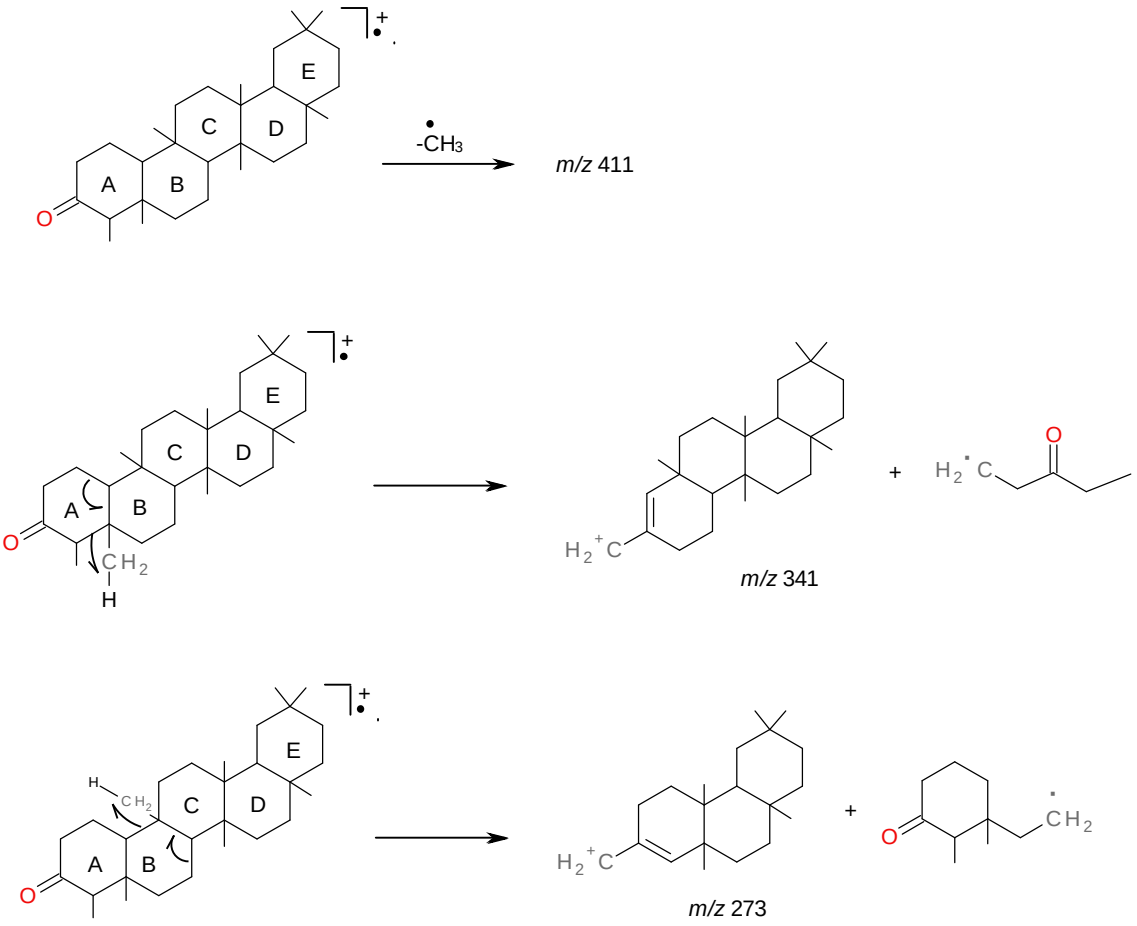

Scheme 3.1

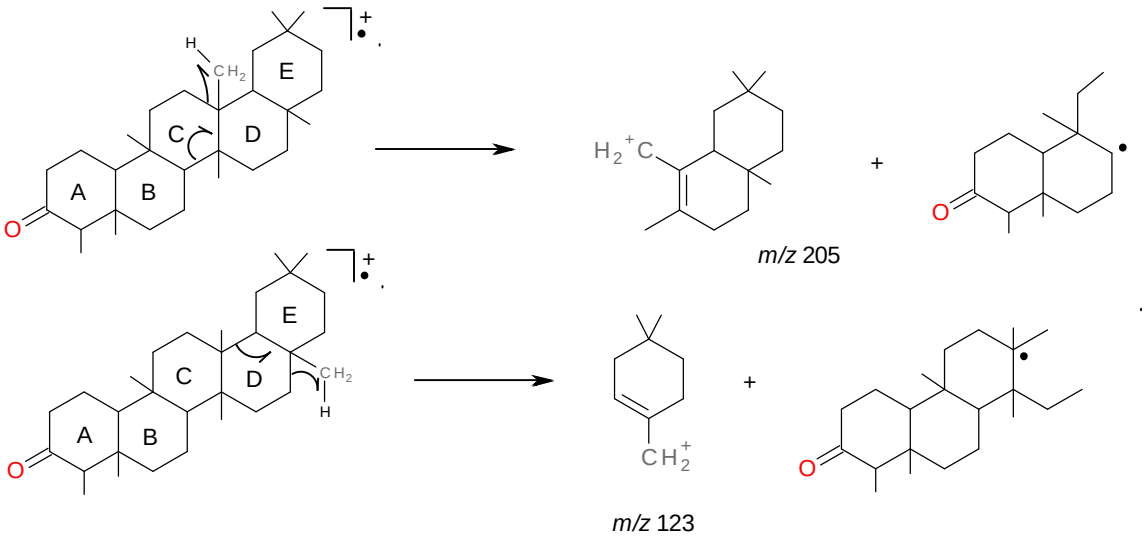
H
CH2
E
C
D
A
B
O
+
H2+C
+
O
m/z 205
E
C
D
CH2
H
A
B
O
+
CH2+
+
O
m/z 123

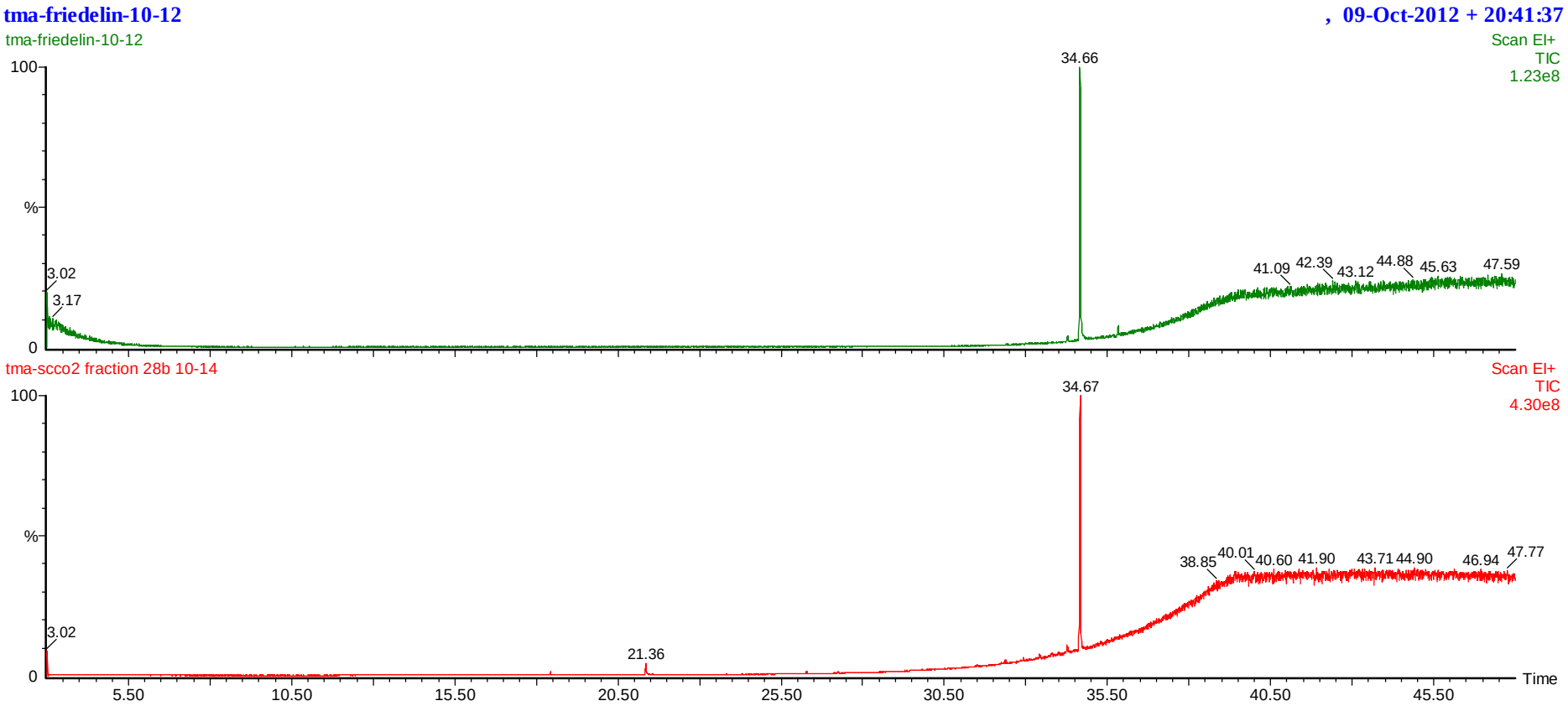

Figure 3.12 GC Chromatogram of a) Friedelin Standard b) Triterpinoid extracted from sugarcane leaves

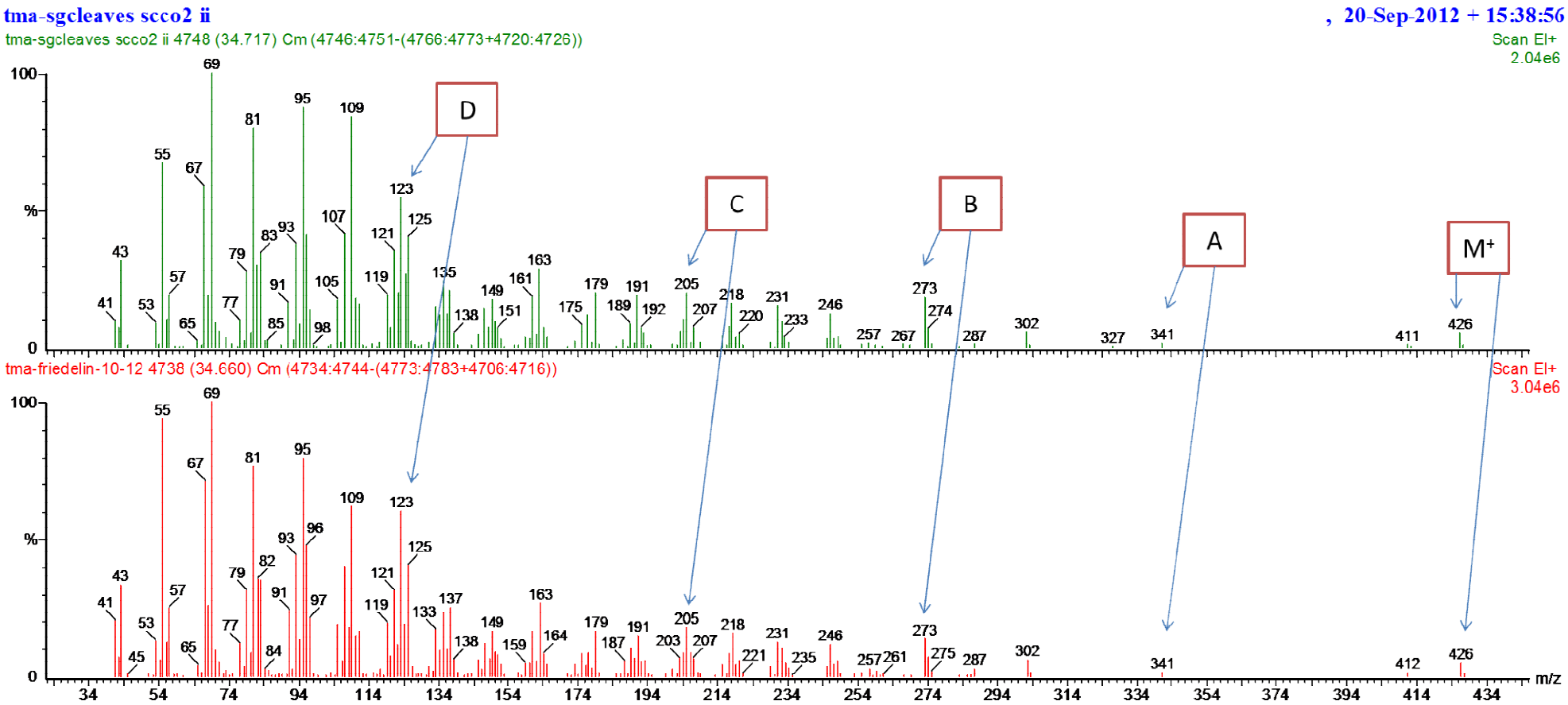

Figure 3.13 EI-Mass spectrum of a) Compound from sugarcane leaves b) friedelin

3.5.3.1.2 ^{13}C NMR

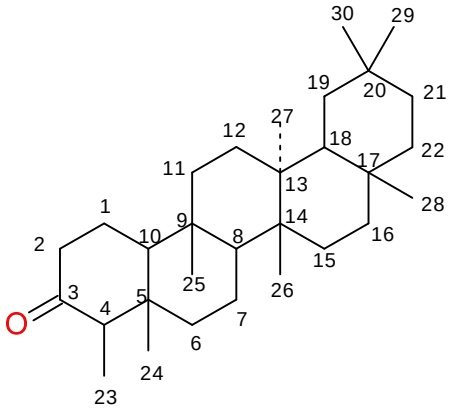

Figure 3.14 Structure of Friedelin

Figure 3.15 shows the ^{13}C NMR spectrum for the compound suspected to be friedelin. The ^{13}C NMR of the Friedelin standard may be viewed in APPENDIX A. The two spectra appear to be consistent. The ^{13}C NMR spectrum for the compound suspected to be friedelin is expanded in Figures 3.16 and 3.17. All the carbon atoms are assigned to their respective signals and are consistent with literature.[22] These are summarised in Table 3.5. From figures 3.15 and 3.17, it can be seen that there are a few impurities present along with friedelin. However the majority of these impurities are also present in the ^{13}C NMR spectrum of the standard which therefore shows that the friedelin extracted from sugarcane wax is relatively pure.

Table 3.5 Carbon signals in the ^{13}C NMR of triterpenoid isolated from sugarcane wax.

Carbon no.	Chemical shift (δ, ppm)
1	22.35
2	41.61
3	213.36
4	58.26
5	42.22
6	41.34
7	18.31
8	53.19
9	37.52

10	59.55
11	35.69
12	30.58
13	39.79
14	38.38
15	32.51
16	36.09
17	30.07
18	42.86
19	35.41
20	28.26
21	32.83
22	39.34
23	6.89
24	14.70
25	18.01
26	20.34
27	18.74
28	32.16
29	31.87
30	35.10

Therefore from the GC, EI-MS and ^{13}C NMR data it can be concluded that this triterpenoid found in the wax extracted from sugarcane leaves is friedelin.

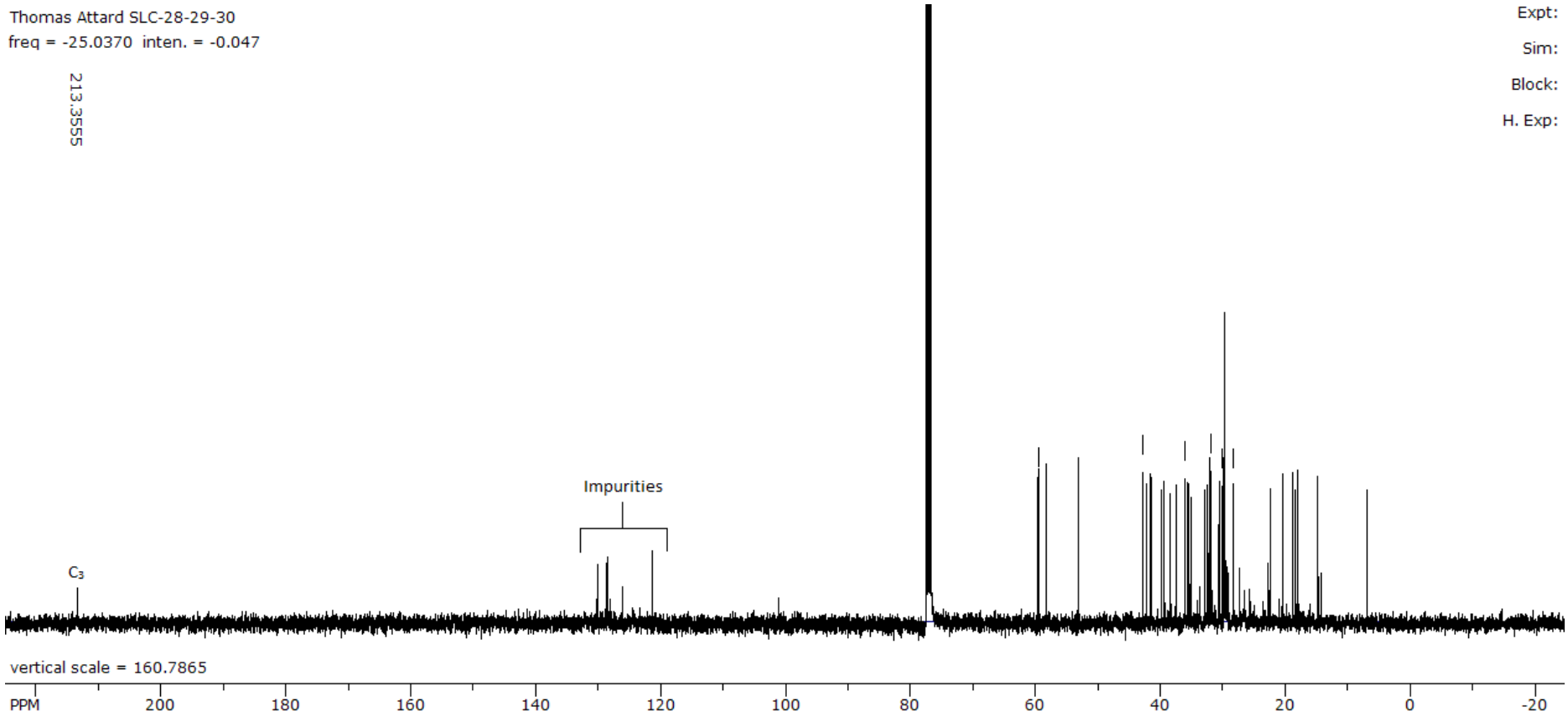

Figure 3.15 ^{13}C spectrum of compound suspected to be friedelin.

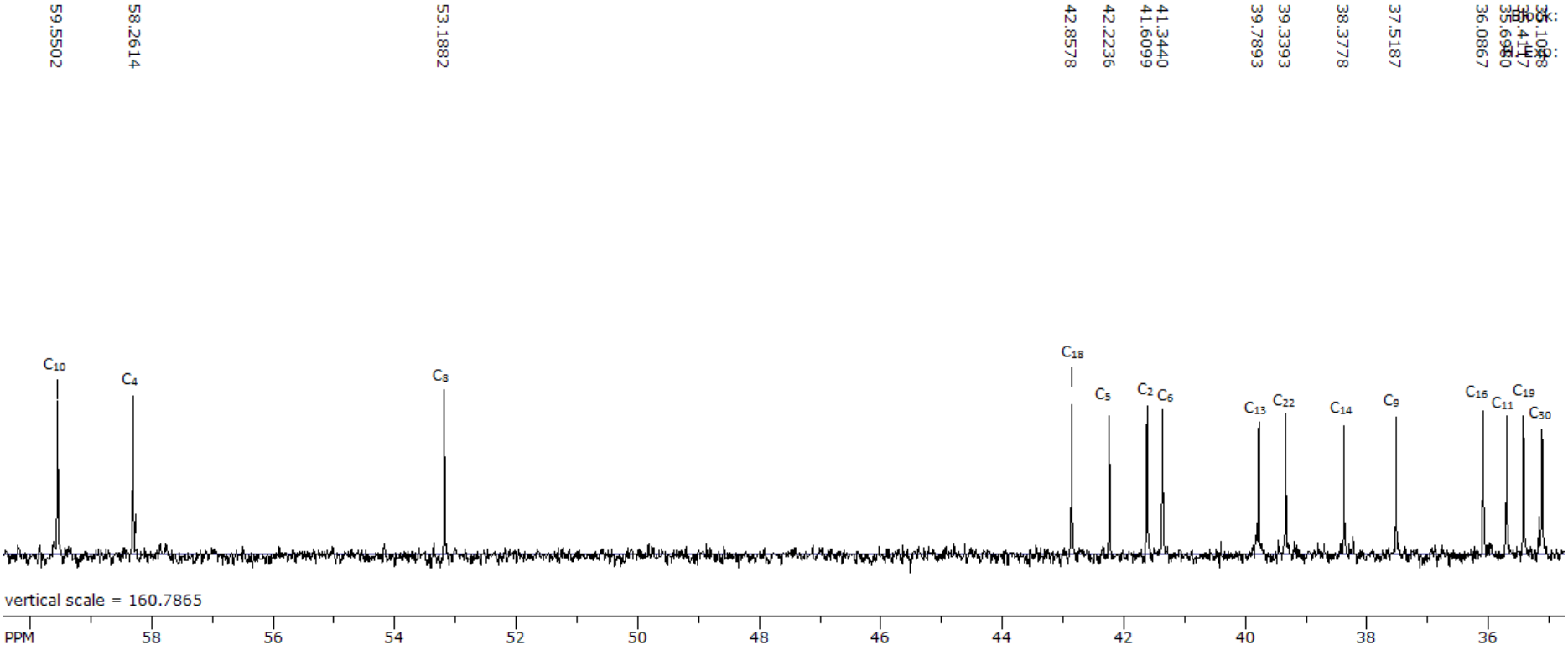

Figure 3.16 ^{13}C NMR spectrum of compound suspected to be friedelin

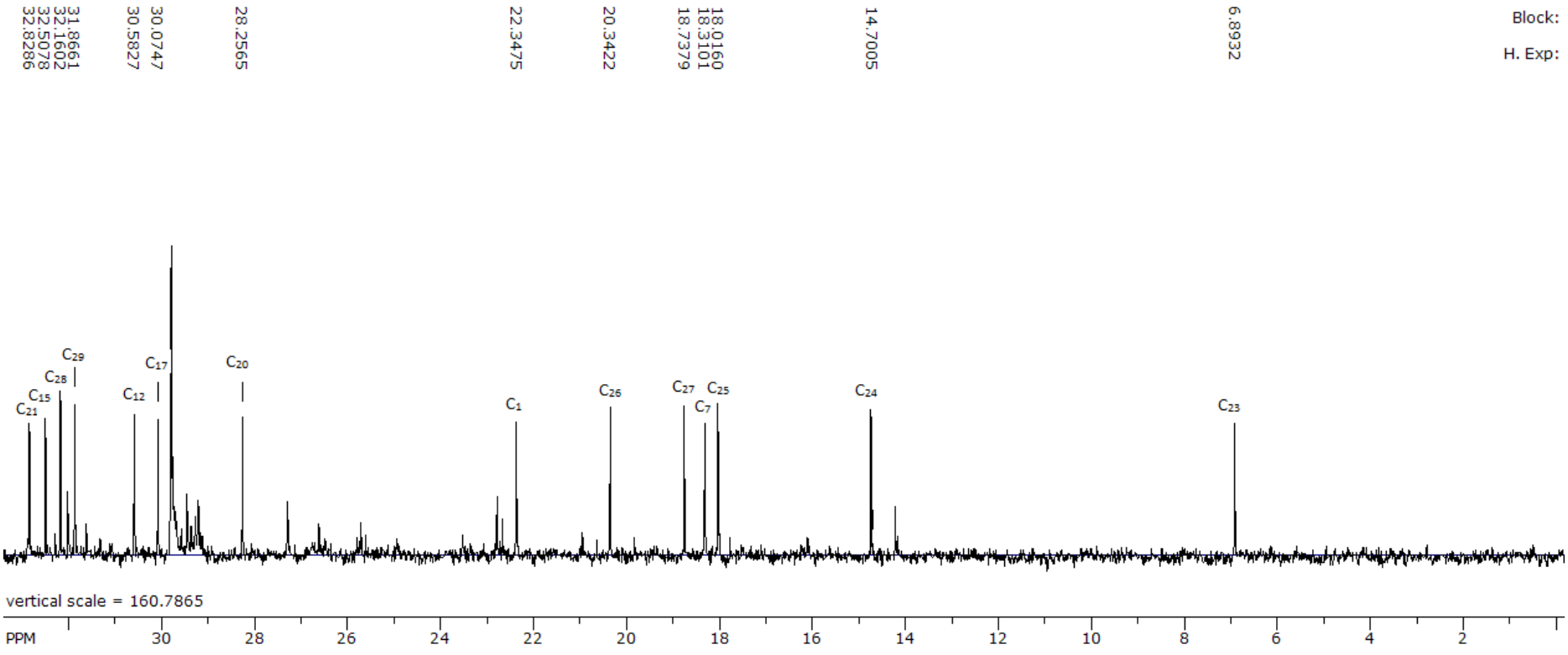

Figure 3.17 ^{13}C NMR spectrum of compound suspected to be friedelin.

3.5.3.2 Simiarenol

Figure 3.19 illustrates the successful isolation of the triterpenoid compound from the crude wax. The compound was analysed by a combination of EI-MS fragmentation data, NIST 2008 library data and ^{1}H and ^{13}C NMR data, all of which give strong evidence to suggest that the compound is simiarenol ($C_{30}H_{50}O$). This is a pentacyclic, hopane-derived triterpene alcohol. Figure 3.18 illustrates the structure of simiarenol.

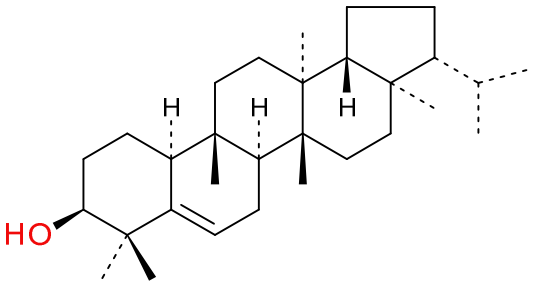

Figure 3.18 Structure of simiarenol

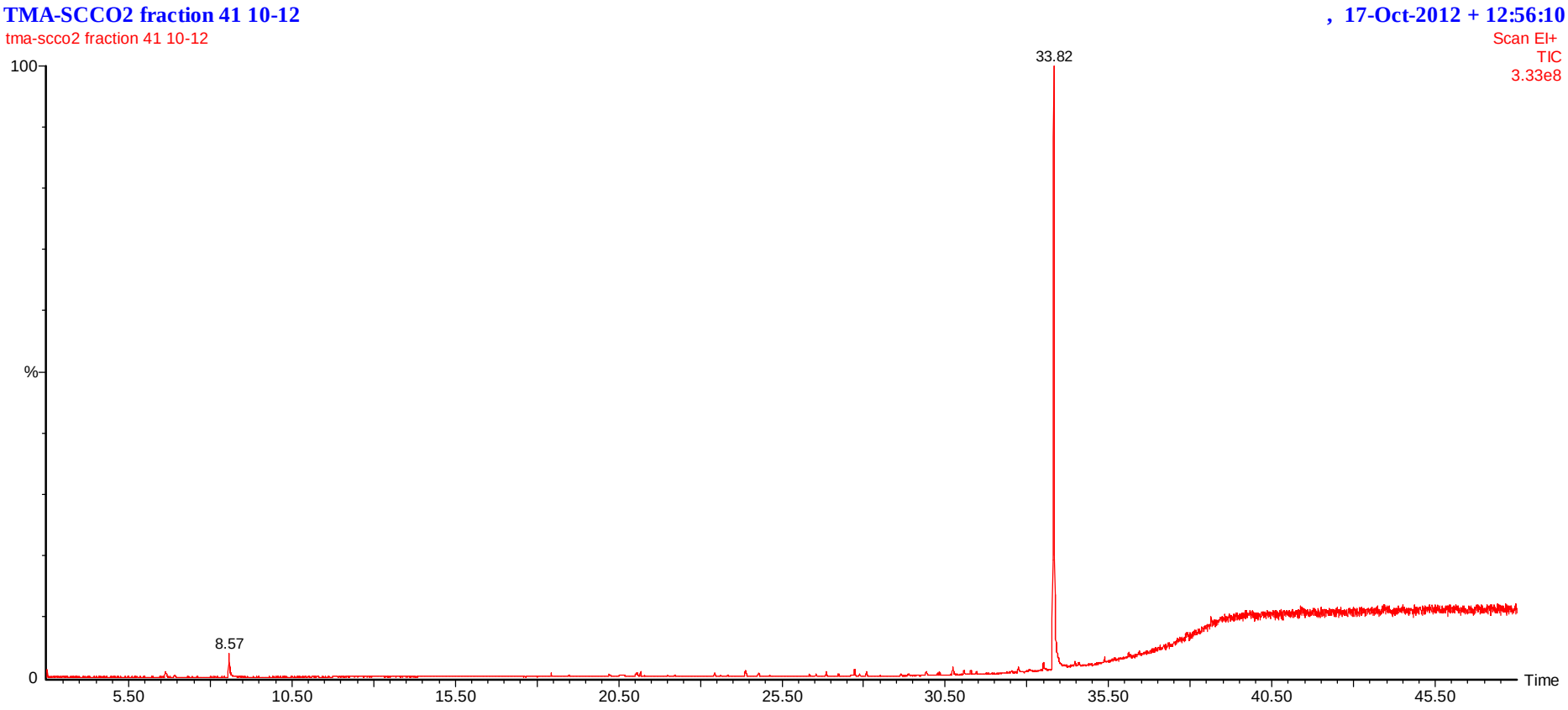

Figure 3.19 GC chromatogram fraction containing triterpenoid that is suspected to be simiarenol

3.5.3.2.1 GC-MS data

Figure 3.20 is the EI-mass spectrum of the compound that is suspected to be simiarenol. Figure 3.21 compares this EI-mass spectrum with that of the NIST 2008 library simiarenol standard. The mass fragmentation patterns of the compound and the standard are very similar. The ion at *m/z* 426 is the molecular ion of simiarenol. Scheme 3.2 illustrates the major fragmentation patterns of simiarenol. The base peak at *m/*z 274 is occurs as a result of a retro-Diels-Alder cleavage of the second ring resulting in species *(a)*.[23] Another major fragment arises at *m/z* 259 (species (*b)* as a result of the loss of the allylic C-26 methyl from species *(a)*. There is an important weak peak at *m/z* 231 (species (*c)*) which arises as a result of the loss of the isopropyl side chain from species (*a)*. This is important as it differentiates the EI-spectrum of simiarenol from another triterpinoid β-glutinol. These two compounds have very similar mass spectra, but the ion at *m/z* 231 is found only in the spectrum of simiarenol as the loss of the isopropyl chain from *m/z* 274 occurs more easily in simiarenol than in β-glutinol. Therefore the EI-mass spectrum of the compound isolated from the crude wax gives strong evidence to suggest that it is simiarenol as it indicates the presence of the isopropyl group (loss of M-43 from *m/z* 274 to give *m/z* 231) as well as the Δ^5 double bond (*m/z* 274). The presence of the weak peak at 231 indicates that the compound in question is not β-glutinol.[23]

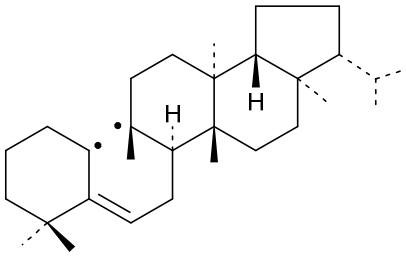

-*e* -*e*

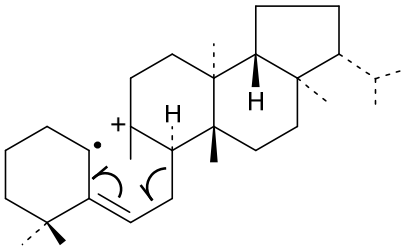

(M$^+$) *m/e* 410

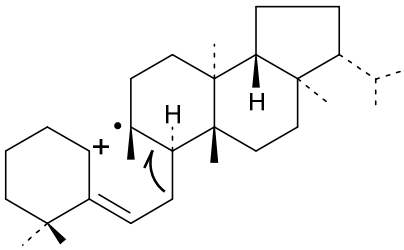

(M$^+$) *m/e* 410

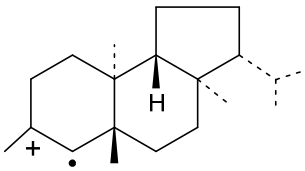

(a)

(M$^+$) *m/e* 274

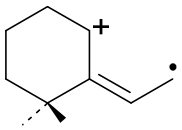

(d)

(M$^+$) *m/e* 136

-$C_3H_7^{\bullet}$

-$Me^{\bullet}$

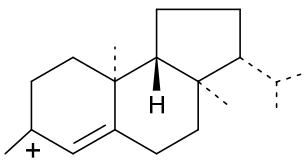

(b)

(M$^+$) *m/e* 259

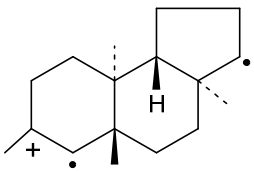

(c)

(M$^+$) *m/e* 231

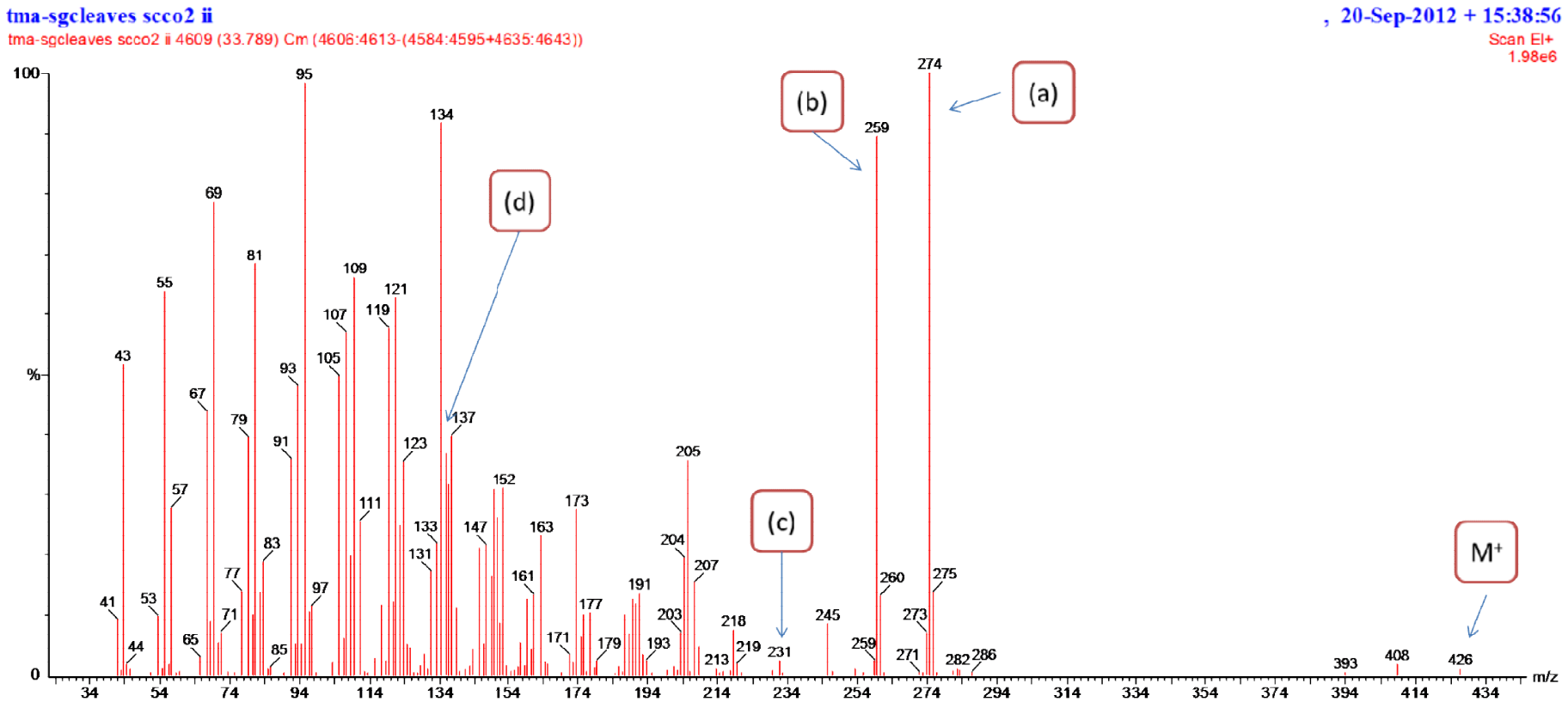

Figure 3.20 EI-Mass spectrum of compound suspected to be simiarenol.

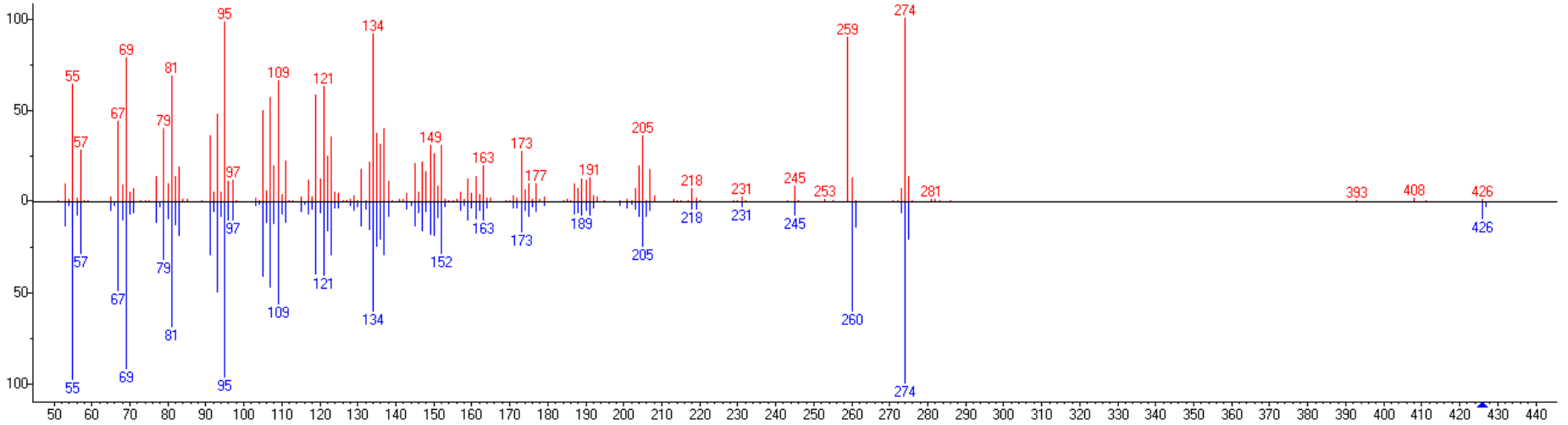

Figure 3.21 Comparison of EI-mass spectrum of unknown compound with simiarenol (NIST)

3.5.3.2.2 ^{13}C NMR

Figure 3.22 is the ^{13}C NMR spectrum obtained for the triterpinoid compound suspected to be simiarenol. The chemical shifts are comparable to those that are found in literature for simiarenol. The two carbon signals at δ 142 and δ 122 indicate the presence of two olefinic carbon atoms (carbon atoms no.5 and no.6) which therefore highlights the presence of an unsaturated double bond in the structure. Another carbon signal which is found in the NMR spectrum of simiarenol and in the NMR spectrum of the unknown compound is a carbon signal at δ 76.5 (found adjacent to the d-chloroform peaks as seen in Figure 3.23 which is an oxygenated carbon signal (carbon atom no.3). This signal indicates the presence of a hydroxyl group attached to the third carbon of the unknown compound. The overall ^{13}C NMR spectrum looks to be consistent with what is found in literature but some discrepancies were found.[24,25] This could be due to the sample being too dilute as well as the type of method employed. In fact there are also discrepancies between different sets of published data for simiarenol.[24,25] However the easily identifiable peaks (describe above) showed good correlation and this therefore gives further evidence to suggest that the structure is simiarenol. However this could only be proven by running a ^{13}C NMR of the pure standard.

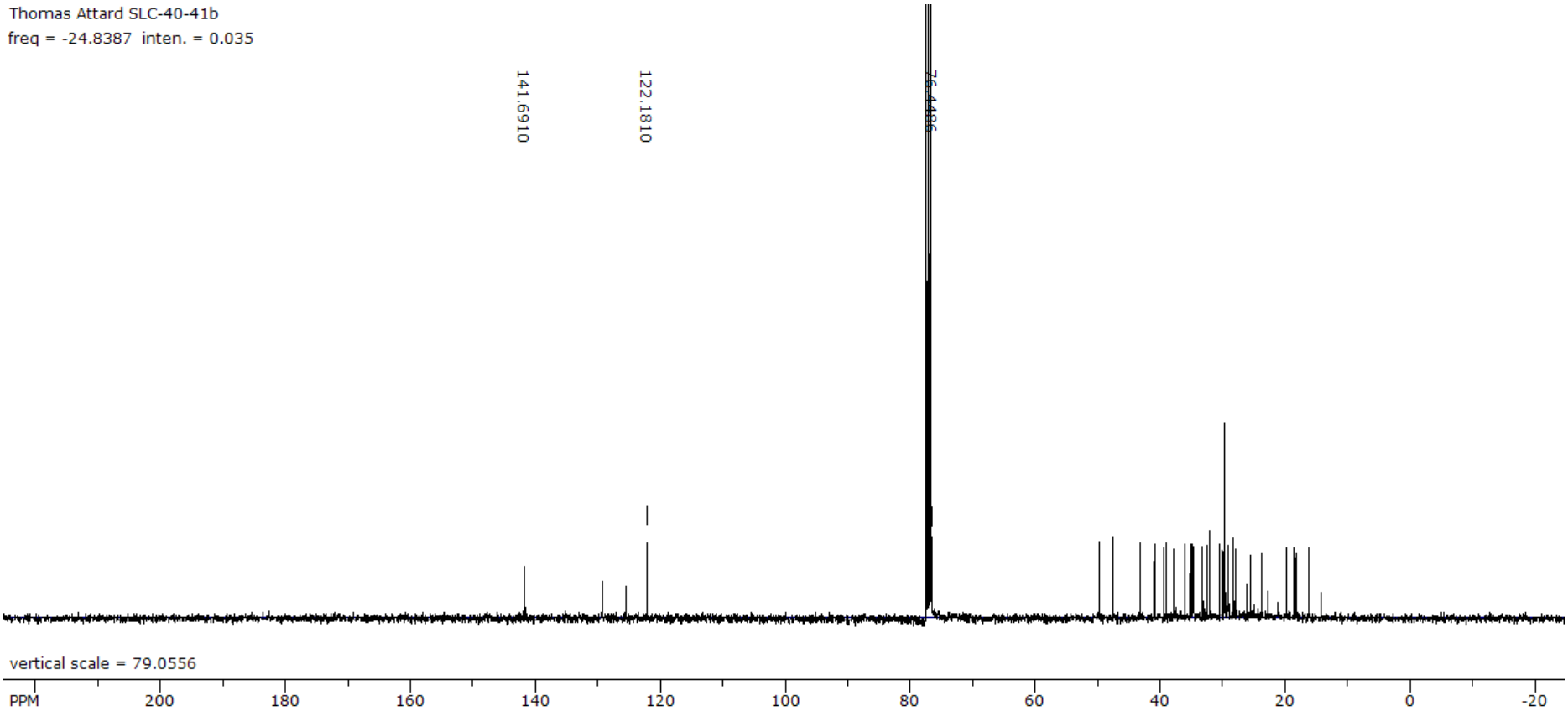

Figure 3.22 ^{13}C NMR of triterpinoid which is thought to be simiarenol.

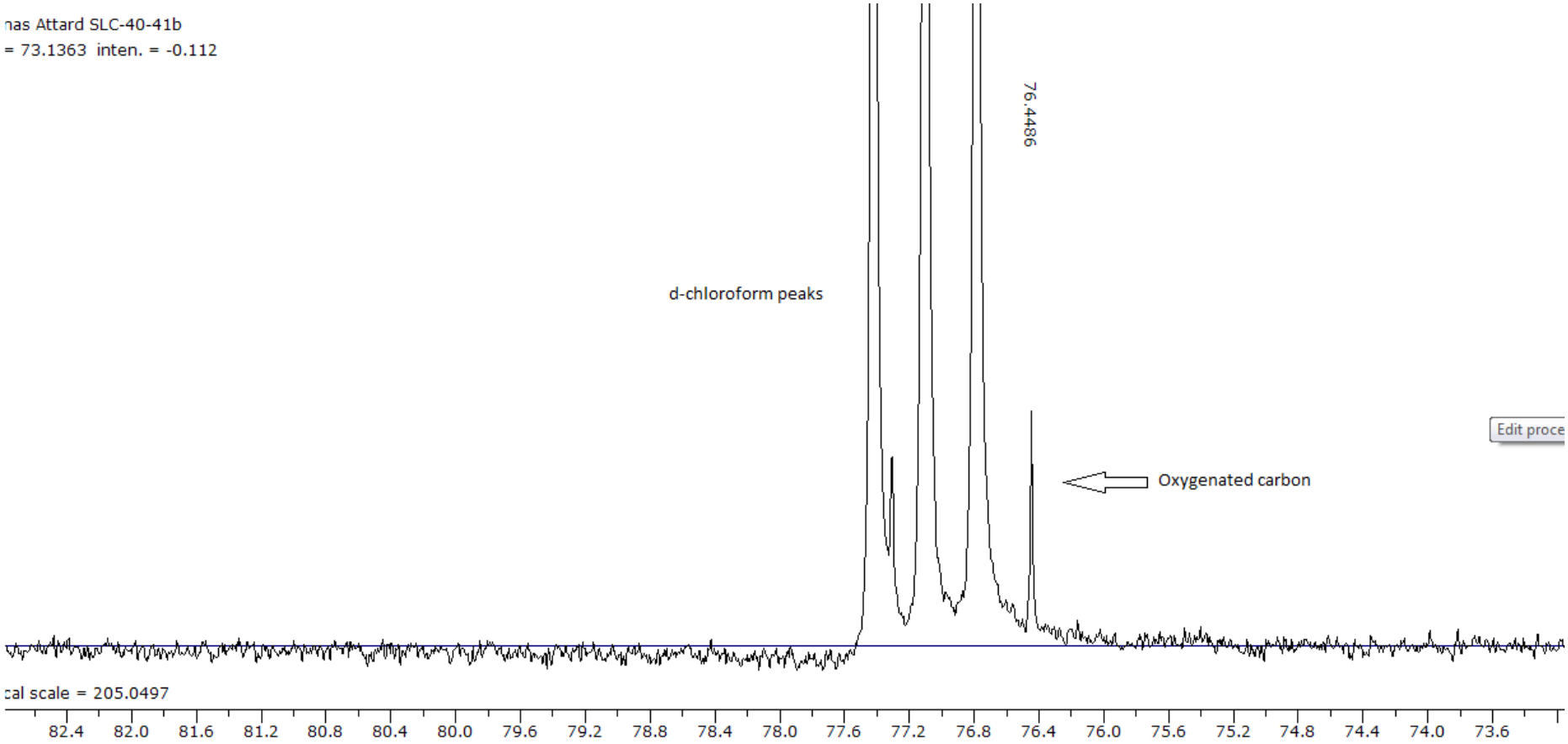

Figure 3.23 ^{13}C NMR indicating the oxygenated carbon.

3.5.3.3 Other Triterpinoids

Unfortunately, as stated previously, the remaining triterpinoids were collected in one fraction together with the long-chain fatty aldehydes. Therefore it was not possible to carry out ^{1}H and ^{13}C NMR. Therefore it was only possible to analyse the compounds using GC-MS data together with the NIST 2008 library data. Therefore further work would involve trying to isolate each triterpenoid in order to carry out further analysis.

Figure 3.24 is a GC chromatogram showing the fraction containing the remaining triterpenoids (labelled as compound 1, 2 and 3). The EI-mass spectra of the three compounds are quite similar and share certain common characteristics (Figure 3.25). They all have a molecular mass of 440 amu (*m/z* 440), as well as two fragments at *m/z* 408 $(M-32)^{+\cdot}$ and *m/z* 393 $[(M-15)-32)]^{+}$. These fragments strongly point to the loss of a methoxy group during fragmentation as a neutral methanol molecule.[26] The fragmentation pattern of each of the three compounds strongly resembles that of triterpene ethers (as will be explained below) and this, together with the characteristics described previously, gives strong evidence to suggest that these three compounds are unsaturated methoxy triterpenoids having the formula $C_{31}H_{52}O$.

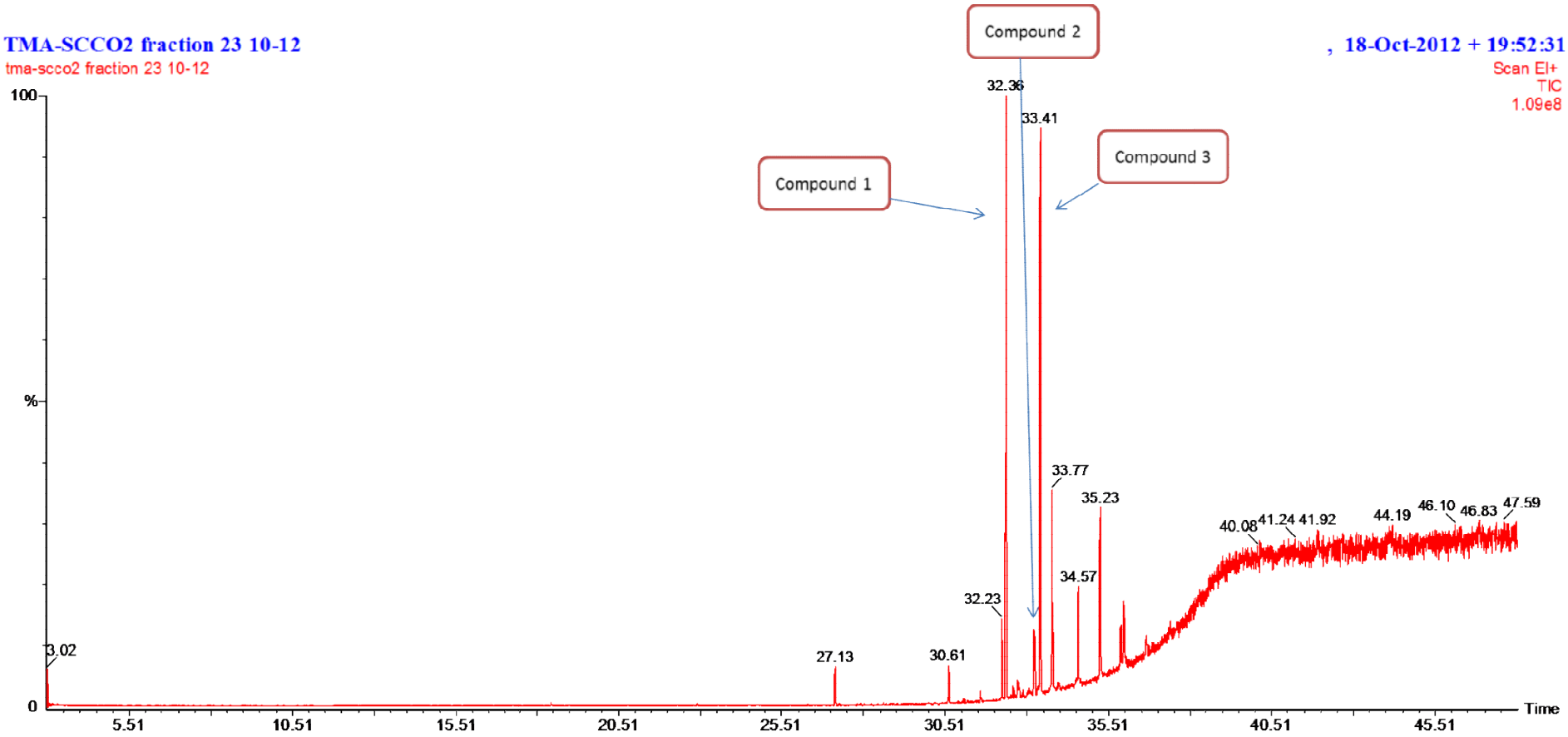

Figure 3.24 GC chromatogram of the fraction containing the three triterpenoids and the free long chain aldehydes.

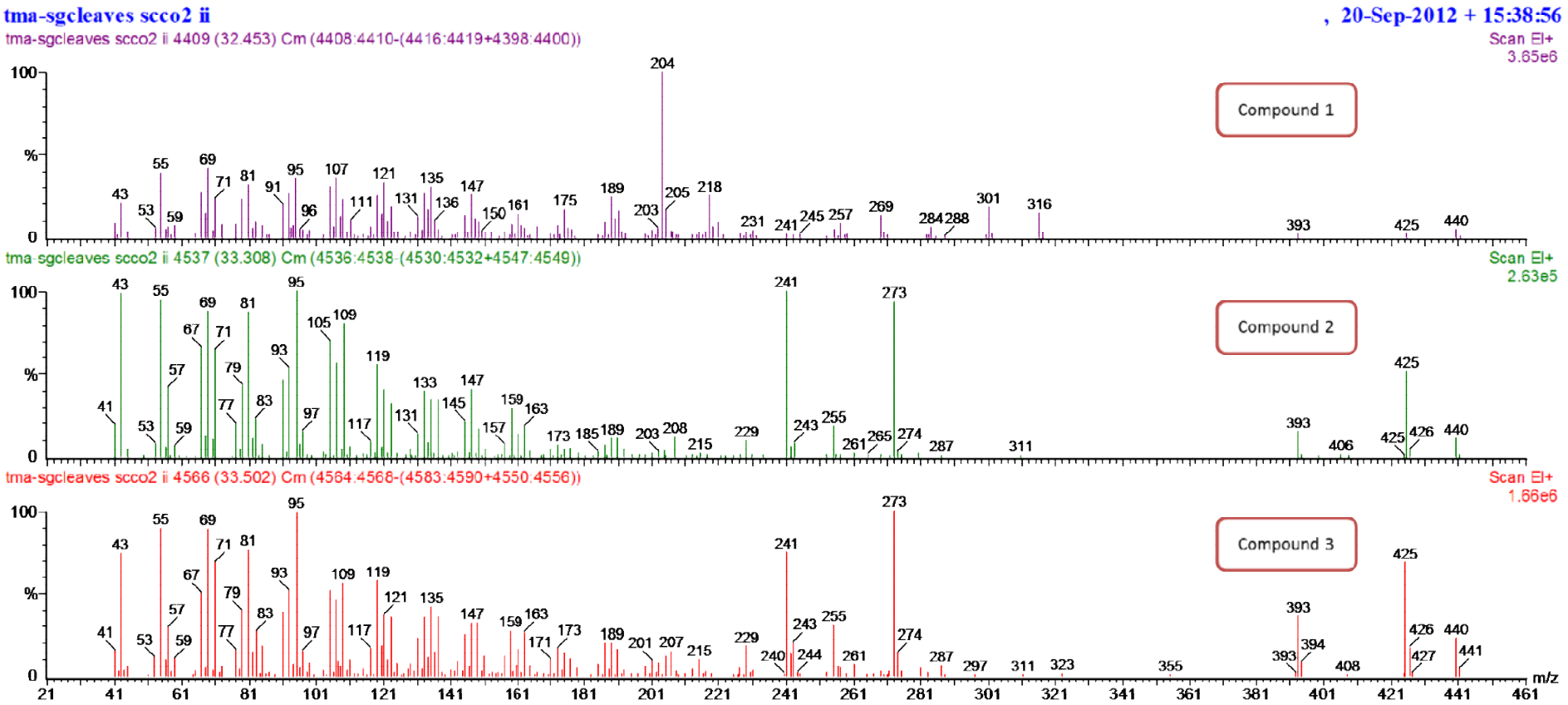

Figure 3.25 EI-Mass Spectra of Triterpenoids : a) compound 1 b) compound 2 c) compound 3

Closer inspection showed that the EI-spectra of compounds 2 and 3 are very similar while that of compound 1 is different. The mass spectrum of compound 1 is dominated by fragments at *m/z* 218, 203 and 189 while the mass spectra of compounds 2 and 3 are dominated by mass fragments at 273 and 241.

3.5.3.3.1 Compound 1

The intense fragments at *m/z* 218, 204 and 189 found in the mass spectrum of compound 1 could be a result of the D/E moiety of normal and D-friedo- triterpenes after C-ring breaking and possible retro-Diels Alder rearrangement.[26] Apart from these fragments, there are other intense peaks at *m/z* 316, 301, 284 and 269. These fragments have been reported by Bryce *et al.* as being typical fragments of crusgallin (Figure 3.26) (taraxer-14-en-3β-ol).[26]

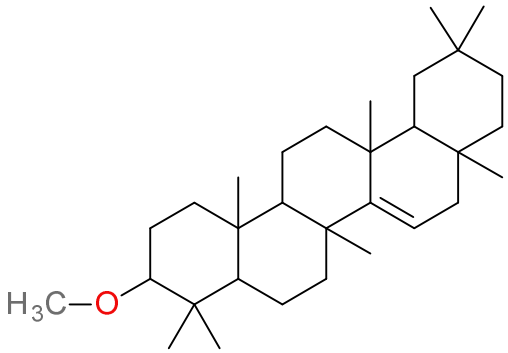

Figure 3.26 Structure of crusgallin

When consulting the NIST 2008 library, it was found that the mass spectrum of crusgallin most resembled the mass spectrum of the compound 1. Furthermore, Bryce *et al.* reported the presence of crusgallin in sugarcane wax.[26] This and the above data indicate that compound 1 could be crusgallin.

3.5.3.3.2 Compounds 2 and 3

Compounds 2 and 3 have very similar mass spectra. The EI mass spectrum of compound 3 is found in Figure 3.27 The major fragment at *m/z* 273 $[M-167]^+$ is characteristic of D:C or E:C-friedo triterpenes of the arborane, bauerane, fernane or multiflorane type having a trisubstituted double bond in the 9(11) position.[27,28] The fragment at *m/z* 241 arises via the loss of methanol from the fragment at *m/z* 273. A very small peak at *m/z* 365 could have arisen as a result of the loss of an isopropyl side-chain from the *m/z* 408 fragment. Therefore this indicates that compounds 2 and 3 are D:C or E:C friedo triterpene methyl ethers having

an isopropyl group on the fifth ring and a tri-substituted double bond in the $\Delta^{9(11)}$ position.[27] Scheme 3.3 illustrates the fragmentation of D:C or E:C- friedo triterpinoids and Table 3.6 summarises the resulting fragments.

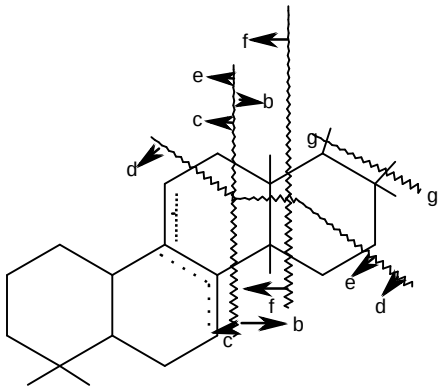

Scheme 3.3

Table 3.6 Comparison of mass spectra of D:C and E:C-Friedo-Triterpenoids

Compound	b-b	c-c	d-d	e-e	f-f	g-g	M^+-15	M^+
2	205	- -	261 229*	273 241*	287 255*	355 323*	425 393*	440
3	205	- -	261 229*	273 241*	287 255*	355 323*	425 393*	440

* Figures shown in the lower line indicate those corresponding to the peak shown in the upper line – MeOH.

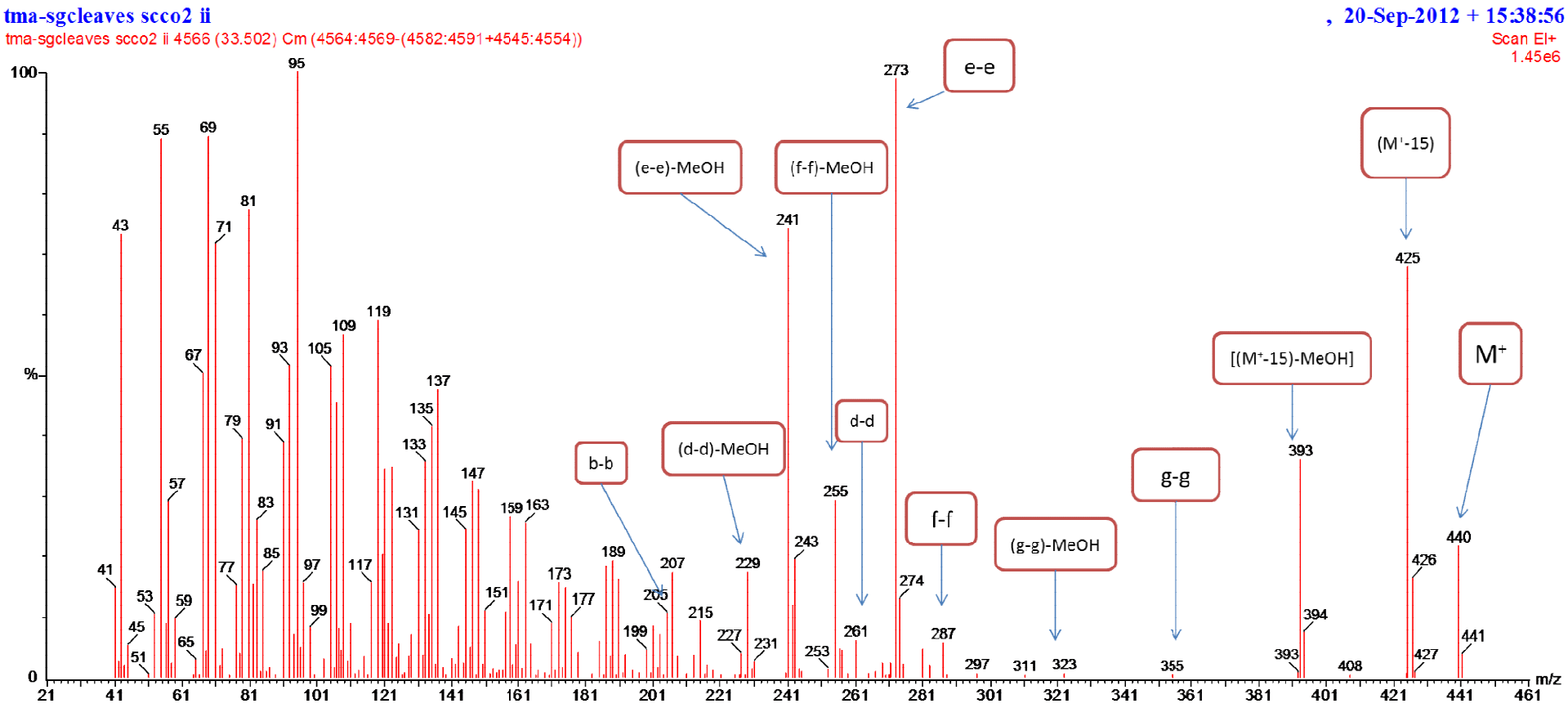

Figure 3.27 EI-Mass spectrum of Compound 3

When consulting NIST, the structure which most resembled the mass spectra of compounds 2 and 3 was found to be arundoin (arbor-9(11)-en-3β-ol ME) which is a D:C friedo-type triterpene methyl ether with a double bond in the 9(11) position. A number of published reports have shown that arundoin is present in the wax extracted from sugarcane along with another D:C friedo-type triterpene methyl ether called cylindrin.[26,29] The mass spectra of cylindrin and arundoin are almost identical. The only difference between the two compounds is the retention times on the GC chromatogram, where arundoin elutes off before cylindrin. Therefore this could suggest that compounds 2 and 3 are arundoin and cylindrin respectively due to the similar mass spectra and the fact that both triterpenoids have already been identified in sugarcane wax. However, this can only be confirmed by: (i) Purchasing pure standards of the compounds in order to directly compare retention times and mass spectra (ii) Isolating the two triterpenoids and analysing them with ^{1}H NMR and ^{13}C NMR.

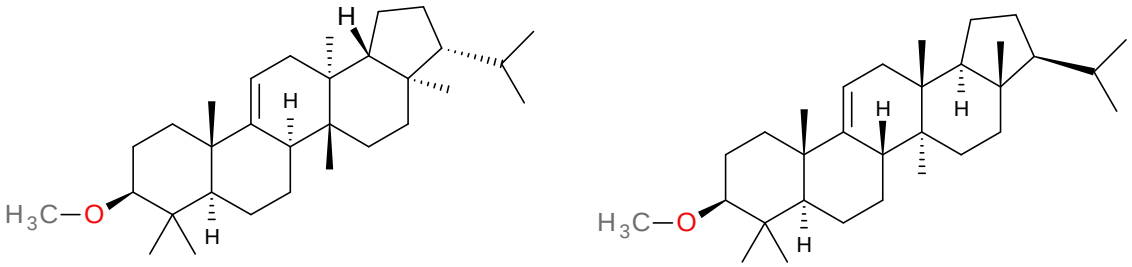

Arundoin Cylindrin

Figure 3.28 Structures of a) Arundoin and b) Cylindrin

4. Experimental

4.1 Supercritical Fluid Extraction

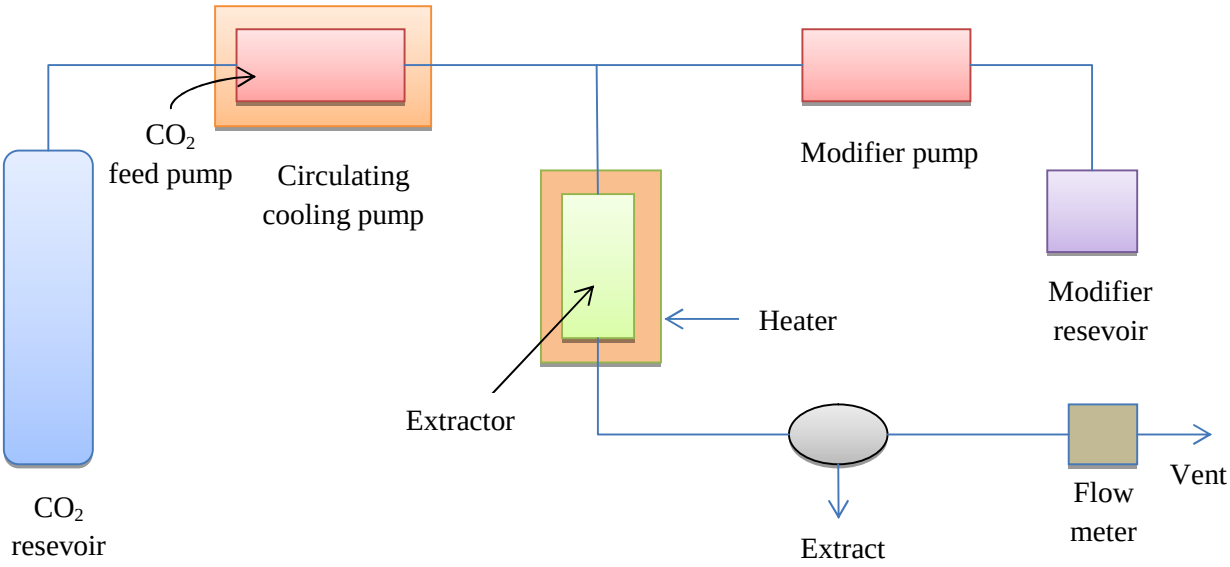

Figure 4.1 Supercritical extraction set-up

The supercritical carbon dioxide extractions were carried out using a SFE-500 provided by Thar technologies. Supercritical fluid grade carbon dioxide (99.99%) was used to conduct the extractions. 100 g of milled biomass (miscanthus, maize or sugarcane bagasse) was placed into the 500 ml extraction vessel and connected to the extraction system. The required temperature and pressure were applied. The reaction vessel was heated to 50 ^{o}C and 5 minutes were allowed for it to equilibrate. An internal pump was used in order to obtain the required pressure (350 bar). The system was run in dynamic mode, in which the carbon dioxide which contained the epicuticular lipids, was allowed to flow into the collection vessel. A flow rate of 40 g min^{-1} of liquid CO_2 was applied and the extraction was carried out for 4 hours. When the extraction was terminated, depressurisation of the system was carried out over a period of 4 hours. The wax was collected by rinsing the collection vessel twice with approximately 100 ml of DCM. The solvent was removed *in vacuo*. The crude wax product was weighed and the % yield was calculated. The results are summarised in the Results section. The plant material was removed and a brush was used to clean the extraction vessel. The system was washed in dynamic mode using a combination of supercritical carbon dioxide and ethanol (10%) for 45 minutes at the extraction pressure. The pump supplying the modifier was then turned off and carbon dioxide was allowed to pass through the system for an additional 20 minutes.

The above procedure was repeated a further five times for each biomass, each time varying the independent variables (temperature and pressure). The reaction conditions for each run are summarised in the following table.

4.2 Flash Chromatography

The crude extract (1 g) was dissolved in 10 ml of DCM in a round bottom flask which contained a small amount of silica gel (high-purity grade for flash chromatography). The solvent was removed under reduced pressure in order to coat the wax onto the silica gel. The mixture was then transferred on top of a 100 g Biotage SNAP HP-Sil cartridge. The flow rate and the equilibration flow rate were set to 50 ml/min. The solvent system employed was hexane (75%) and ethyl acetate (25%). A step gradient system was selected in which the various solvent concentrations were typically changed in large increments and summarised in Table 4.1. The eluent was collected in 15 ml fractions.

Table 4.1 Step Gradient system

Gradient	Solvents	Mix.	Length (CV)
Equil.	Hexane/ethyl acetate	6%	3.0
1	Hexane/ethyl acetate	6%	1.0
2	Hexane/ethyl acetate	6 – 42%	8.1
3	Hexane/ethyl acetate	42 – 50%	1.8
4	Hexane/ethyl acetate	50%	2.0
5	Hexane/ethyl acetate	50 – 57%	1.4
6	Hexane/ethyl acetate	57 – 60%	0.5
7	Hexane/ethyl acetate	60%	1.0
8	Hexane/ethyl acetate	60 – 64%	0.5
9	Hexane/ethyl acetate	64 – 95%	1.4
10	Hexane/ethyl acetate	95 – 100%	1.0
11	Hexane/ethyl acetate	100%	2.0
12	Hexane/ethyl acetate	100%	5.2

5. Conclusion

The optimal conditions for miscanthus giganteus were found to be 350 bar and 50 ^{o}C. For maize, the optimal conditions were found to be 400 bar and 65 ^{o}C while the optimal conditions for sugarcane bagasse were found to be 325 bar and 57 ^{o}C. Results indicate that for miscanthus and sugarcane bagasse, density plays a more important role than temperature in the extraction of waxes. Furthermore, in both cases, the results suggest that a specific density is requited for optimal extraction. In the case of maize, results indicate that temperature is more important than density in the extraction of waxes.

In addition to optimisation, fractionation of sugarcane bagasse and sugarcane leaves is reported. The sugarcane bagasse was fractionated using a number of different fractional separators set at different pressures and temperatures, each having a different pressure. The fractionation of sugarcane leaves was attempted by a combination of complementary chromatographic techniques, namely TLC and flash chromatography.

6. References

1. H. A. Eckert, B. L. Knutson and P. G. Debenedetti, *Nature*, 1996, **383**, 313-318.
2. A. A. Clifford, *Fundamentals of Supercritical Fluids*, Oxford University Press, Oxford, 1998.
3. A. Demirbas, *Energy Convers. Manage.*, 2001, **42**, 279-294.
4. R. S. Oakes, A. A. Clifford and C. M. Rayner, *J. Chem. Soc., Perkin Trans.*, 2001, **1**, 917-941.
5. R. Noyori, *Chem. Rev.*, 1999, **99**, 353–354.
6. E. D. Ramsey, *Analytical Supercritical Fluid Extraction Techniques*, Springer, UK, 1998.
7. S. K. Kumar and K. P. Johnston, *J. of Supercritical Fluids*, 1988, **1**, 15 – 22.
8. M. E. Paulaitis, V. J. Krukonis, R. T. Kurnik, and R. C. Reid, *Rev. Chem. Eng.*, 1983, **1,** 179 – 250.
9. H. Ebeling and E. U. Frenck, *Ber. Bunsenges. Phys. Chem.*, ***88***, 859-*862.*
10. K. P. Johnston, C. A. Eckert, *AlChE J.*, 1981, **27**, 773 – 779.
11. G. A. M. Diepen and F. E. C. Scheffer, *J. Phys. Chem.,* 1953, **57**, 575 – 577.
12. K. P. Johnston, D. H. Ziger and C. A. Eckert, *Ind. Eng. Chem. Fundam.,* 1982, **21**, 191 – 197.
13. R. T. Kurnik S. J. Holla and R. C. Reid. *Chem. Eng. Data,* 1981, **26,** 47 – 51.
14. W. Leitner, *Nature*, 2000, **405**, 129-130.

15. R. L. Mendes, B. P. Nobre, M. T. Cardoso, A. P. Pereira and A. F. Palavra, *Inorganica Chimica Acta,* 2003, **356**, 328 – 334.
16. M. Fettori, N. R. Bulley, A. Meisen, *J. Agric. Food Chem.*, 1987, **35**, 738
17. Balker, *Chem. Rev.*, 1999, **99**, 453 – 473.
18. J. M. Dobbs and K. P. Johnston, *Ind. Eng. Chem. Res.*, 1987, **26**, 1476 – 1482.
19. J. M. Dobbs, J. M. Wong, R. J. Lahiere and K. P. Johnston, *Ing. Eng. Chem. Res.*, 1987, **26**, 56 – 65.
20. A. G. Gonzalez, *Anal. Chim. Acta.*, 1998, **360**, 227 – 241.
21. M. Kane, J. R. Dean and S. M. Hitchen, *Anal. Chim. Acta.*, 1993, **271**, 83 – 90.
22. H. E. Gottlieb, P. A. Ramaiah and D. Lavie, *Magn. Reson. Chem.*, 1985, **23**, 616 – 620.
23. R. T. Aplin, H. R. Arthur and W. H. Hui, *J. Chem. Soc. C.*, 1966, **0**, 1251 – 1255.
24. A. K. Chakravarty, *Tetrahedron*, 1994, **50**, 2865 – 2876.
25. N. Hee Yoo, D. Sik Jang and J. Sook Kim, *J. Korean Soc. Appl. Biol. Chem.*, 2008, **51**, 305 – 308.
26. T. A. Bryce, M. Martin-Smith, G. Osske, K. Schreiber and G. Subramanian, *Tetrahedron*, **23**, 1283 – 1296.
27. K. Nishimoto, M. Ito and S. Natori, *Tetrahedron*, 1968, **24**, 735 – 752.
28. K. Shiojima, Y. Arai, K. Masuda, Y. Takase, T. Ageta and H. Ageta, *Chem. Pharm. Bull.*, 1992, **40**, 1683 – 1690.
29. G. Nuissier, P. Bourgeois, M. Grignon-Dubois, P. Pardon and M. H. Lescure, *Phytochem.*, 2002, **61**, 721 – 726.